

P
JOURNAL
OF
FOOD
PROCESS
ENGINEERING

D.R. HELDMAN
and
R.P. SINGH
COEDITORS

FOOD & NUTRITION
PRESS, INC.

VOLUME 20, NUMBER 5

NOVEMBER 1997

2

JOURNAL OF FOOD PROCESS ENGINEERING

Editor: **D.R. HELDMAN**, 214 Agricultural/Engineering Building,
University of Missouri, Columbia, Missouri
R.P. SINGH, Agricultural Engineering Department, University of
California, Davis, California

Editorial

Board:

J.M. AGUILERA, Santiago, Chile
G. BARBOSA-CANOVAS, Pullman, Washington
S. BRUIN, Vlaardingen, The Netherlands
M. CHERYAN, Urbana, Illinois
P. CHINACHOTI, Amherst, Massachusetts
J.P. CLARK, Chicago, Illinois
A. CLELAND, Palmerston North, New Zealand
M. ETZEL, Madison, Wisconsin
R. HARTEL, Madison, Wisconsin
F.-H. HSIEH, Columbia, Missouri
K.H. HSU, E. Hanover, New Jersey
M.V. KARWE, New Brunswick, New Jersey
E.R. KOLBE, Corvallis, Oregon
J. KROCHTA, Davis, California
L. LEVINE, Plymouth, Minnesota
M. McCARTHY, Davis, California
S. MULVANEY, Ithaca, New York
H. RAMASWAMY, St. Anne Bellevue PQ, Canada
M.A. RAO, Geneva, New York
T. RUMSEY, Davis, California
Y. SAGARA, Tokyo, Japan
S.K. SASTRY, Columbus, Ohio
E. SCOTT, Blacksburg, Virginia
K.R. SWARTZEL, Raleigh, North Carolina
A.A. TEIXEIRA, Gainesville, Florida
G.R. THORPE, Melbourne, Victoria, Australia
H. WEISSER, Freising-Weihenstephan, Germany

All articles for publication and inquiries regarding publication should be sent to DR. D.R. HELDMAN, COEDITOR, *Journal of Food Process Engineering*, University of Missouri-Columbia, 214 Agricultural Engineering Bldg., Columbia, MO 65211 USA; or DR. R.P. SINGH, COEDITOR, *Journal of Food Process Engineering*, University of California, Davis, Department of Agricultural Engineering, Davis, CA 95616 USA.

All subscriptions and inquiries regarding subscriptions should be sent to Food & Nutrition Press, Inc., 6527 Main Street, P.O. Box 374, Trumbull, CT 06611 USA.

One volume of six issues will be published annually. The price for Volume 20 is \$164.00, which includes postage to U.S., Canada, and Mexico. Subscriptions to other countries are \$187.00 per year via surface mail, and \$198.00 per year via airmail.

Subscriptions for individuals for their own personal use are \$134.00 for Volume 20, which includes postage to U.S., Canada and Mexico. Personal subscriptions to other countries are \$157.00 per year via surface mail, and \$168.00 per year via airmail. Subscriptions for individuals should be sent directly to the publisher and marked for personal use.

The *Journal of Food Process Engineering* is listed in *Current Contents/Agriculture, Biology & Environmental Sciences (CC/AB)*, and *SciSearch*, and *Research Alert*.

The *Journal of Food Process Engineering* (ISSN:0145-8876) is published (February, April, June, August, October and December) by Food & Nutrition Press, Inc.—Office of Publication is 6527 Main Street, P.O. Box 374, Trumbull, Connecticut 06611 USA.

Second class postage paid at Bridgeport, CT 06602.

POSTMASTER: Send address changes to Food & Nutrition Press, Inc., 6527 Main Street, P.O. Box 374, Trumbull, Connecticut 06611 USA.

JOURNAL OF FOOD PROCESS ENGINEERING

JOURNAL OF FOOD PROCESS ENGINEERING

Editor: **D.R. HELDMAN**, 214 Agricultural/Engineering Building, University of Missouri, Columbia, Missouri
R.P. SINGH, Agricultural Engineering Department, University of California, Davis, California

Editorial Board:

J.M. AGUILERA, Univ. Catolica, Department of Chemical Engineering, P.O. Box 6177, Santiago, Chile
G. BARBOSA-CANOVAS, Washington State University, Department of Biosystems Engineering, 207 Smith Ag Building, Pullman, Washington 99164
S. BRUIN, Unilever Research Laboratory, Vlaardingen, The Netherlands
M. CHERYAN, 110 Agricultural Bioprocess Laboratory, University of Illinois, 1302 West Pennsylvania Ave., Urbana, Illinois 61801
P. CHINACHOTI, University of Massachusetts, Department of Food Science, Chenoweth Lab, Amherst, Massachusetts 01003
J.P. CLARK, Fluor Daniel, 200 West Monroe St., Chicago, Illinois 60606
A. CLELAND, Department of Food Technology, Massey University, Palmerston North, New Zealand
M. ETZEL, University of Wisconsin, Department of Food Science, Babcock Hall, Madison, Wisconsin 53706
R. HARTEL, University of Wisconsin, Department of Food Science, Babcock Hall, Madison, Wisconsin 53706
F.-H. HSIEH, Departments of Biological & Agricultural Engineering and Food Science & Human Nutrition, University of Missouri, Columbia, Missouri 65211
K.H. HSU, RJR Nabisco, Inc., P.O. Box 1944, E. Hanover, New Jersey 07936
M.V. KARWE, Rutgers, The State University of New Jersey, P.O. Box 231, Center for Advanced Food Technology, New Brunswick, New Jersey 08903
E.R. KOLBE, Oregon State University, Dept. of Bioresource Engineering and Food Science & Technology, Gilmore Hall 200, Corvallis, Oregon 97331-3906
J. KROCHTA, Department of Food Science & Technology, University of California, Davis, California 95616
L. LEVINE, Leon Levine & Associates, 2665 Jewel Lane, Plymouth, MN 55447
M. McCARTHY, Biological and Agricultural Engineering Department, University of California, Davis, California 95616
S. MULVANEY, Cornell University, Department of Food Science, Stocking Hall, Ithaca, New York 14853-7201
H. RAMASWAMY, Macdonald Campus of McGill, Dept. of Food Science & Agricultural Chemistry, 21111 Lakeshore Rd., St. Anne Bellevue PQ, H9X 3V9, Canada
M.A. RAO, Department of Food Science and Technology, Institute for Food Science, New York State Agricultural Experiment Station, Geneva, New York 14456
T. RUMSEY, Biological and Agricultural Engineering Department, University of California, Davis, California 95616
Y. SAGARA, Department of Agricultural Engineering, Faculty of Agriculture, The University of Tokyo, 1-1-1 Yayoi, Bunkyo-ku, Tokyo 113, Japan
S.K. SASTRY, Agricultural Engineering Department, Ohio State University, 590 Woody Hayes Dr., Columbus, Ohio 43210
E. SCOTT, Department of Mechanical Engineering, Virginia Polytechnic Institute and State University, Blacksburg, Virginia 24061
K.R. SWARTZEL, Department of Food Science, North Carolina State University, Box 7624, Raleigh, North Carolina 27695-7624
A.A. TEIXEIRA, Agricultural Engineering Department, University of Florida, Frazier Rogers Hall, Gainesville, Florida 32611-0570
G.R. THORPE, Department of Civil and Building Engineering, Victoria University of Technology, P.O. Box 14428 MCMC, Melbourne, Victoria, Australia 8000
H. WEISSER, University of Munich, Inst. of Brewery Plant and Food Packaging, D 85350 Freising-Weihenstephan, Germany

Journal of FOOD PROCESS ENGINEERING

**VOLUME 20
NUMBER 5**

**Coeditors: D.R. HELDMAN
R.P. SINGH**

**FOOD & NUTRITION PRESS, INC.
TRUMBULL, CONNECTICUT 06611 USA**

© Copyright 1997 by
Food & Nutrition Press, Inc.
Trumbull, Connecticut 06611 USA

All rights reserved. No part of this publication may be reproduced, stored in a retrieval system or transmitted in any form or by any means: electronic, electrostatic, magnetic tape, mechanical, photocopying, recording or otherwise, without permission in writing from the publisher.

ISSN 0145-8876

Printed in the United States of America

CONTENTS

Moisture Sorption Isotherms for Karingda (<i>Citrullus lanatus</i> (Thumb) Mansf) Seed, Kernel and Hull S.H. SUTHAR and S.K. DAS	349
Inactivation Kinetics of <i>Salmonella dublin</i> by Pulsed Electric Field I. SENSOY, Q.H. ZHANG and S.K. SASTRY	367
Textural and Viscoelastic Changes of Canned Biscuit Dough During Microwave and Conventional Baking B. PAN and M.E. CASTELL-PEREZ	383
Analysis of Mass Transfer in Osmotic Dehydration Based on Profiles of Concentration, Shrinkage, Transmembrane Flux and Bulk Flow Velocity in the Domain of Time and Space Z. YAO and M. LE MAGUER	401
The Thermal Properties of Potatoes and Carrots as Affected by Thermal Processing E.G. MURAKAMI	415

30 MAR 2011

MOISTURE SORPTION ISOTHERMS FOR KARINGDA (*CITRULLUS LANATUS* (THUMB) MANSF) SEED, KERNEL AND HULL

S.H. SUTHAR¹ and S.K. DAS²

Post Harvest Technology Centre
Department of Agricultural and Food Engineering
Indian Institute of Technology
Kharagpur-721302 (India)

Accepted for Publication December 2, 1996

ABSTRACT

Adsorption-desorption behaviors of karingda (Citrullus lanatus (Thumb) Mansf) seed, kernel and hull for nine equilibrium relative humidities (ERH) ranging between 11 and 96% at temperatures of 10, 20, 30, 40 and 50C were studied following a static equilibration technique using saturated solutions of various salts. Under both the adsorption and desorption processes, the equilibrium moisture contents (EMC) of the hull were found to be highest followed by those of the seed and the kernel at all the corresponding temperatures and ERH values. Analysis of these data using four sorption models (modified Henderson, modified Halsey, modified Chung-Pfost and Guggenheim-Anderson-de Boer) and taking the temperature dependence of the respective coefficient into consideration, it revealed that both the Chung-Pfost and the GAB models were acceptable in describing EMC-ERH relationships for karingda seed, kernel and hull over the entire range of temperatures. The excess heat of sorption of all the samples, estimated from the Clausius-Clapeyron equation, decreased exponentially with the increase in moisture content of the same.

INTRODUCTION

Karingda (*Citrullus lanatus* (Thumb) Mansf) belongs to Cucurbitaceae family which is probably an ancestral type of watermelon. It is largely grown in western and northern India as a single or mixed crop with pearl-millet or

¹ Present address: Rural Engineering Department, Gujarat Agricultural University, S.K. Nagar (B.K.)-385506 (India).

² To whom correspondence should be made: Dr. S.K. Das, Post Harvest Technology Centre, Department of Agricultural and Food Engineering, Indian Institute of Technology, Kharagpur-721302 (India).

sorghum in both summer and rainy seasons (Joshi 1990) with an average yield of green fruit of 8000-12000 kg/ha (Singh 1983). The immature fruit is usually consumed as a vegetable while the whole or intact kernels, obtained by dehulling the matured seeds and traditionally known as *magaz*, have a large demand as an adjunct or condiment to many Indian sweetmeat and savory food items (Joshi 1990). The annual production of *karingda* seed is reported to be about 0.2 million tonne (Joshi 1990). The kernel contains about 38% protein and 47% crude fat. The *karingda* seed oil is highly unsaturated containing 67.3% linoleic and 11.1% oleic acids (unpublished data).

Moisture content is an important parameter that influences the storability, handling, and processing of agricultural seeds. The moisture content of freshly harvested *karingda* seeds is in the range of 35-40% (w.b.). This moisture needs to be brought down to about 6% d.b. level for safe storage and subsequent uses. Mechanical drying of agricultural seeds using warm, low relative humidity air is generally preferred to natural sun drying for obtaining better and uniform quality products within a reasonable period of time. Owing to the hygroscopic nature of cucurbita seeds and their kernels (Akritidis *et al.* 1988; Ezeike 1988), storing them under unfavorable conditions leads to adsorption of moisture from the surrounding that accelerates the growth of undesirable microorganisms and insects, development of free fatty acids in the extracted oil and deterioration of edible quality of the kernels (Mazza and Jayas 1991). The hardness of the hulls of various agricultural seeds has been reported to be largely dependent to their moisture contents (Ezeike 1986). Dehulling of many oil bearing seeds is considered to be affected by their moisture contents in equilibrium with their surroundings. Some workers (Joshi 1993; Teotia and Ramakrishna 1984; Subramanian *et al.* 1990) have recently reported that proper moisture conditioning is one of the decisive parameters for mechanical dehulling of pumpkin, melon and sunflower seeds to obtain a reasonably high percent yield of whole or intact kernels.

Undoubtedly, a knowledge of equilibrium moisture content (EMC) and equilibrium relative humidity (or water activity of foods) relationships at various temperatures and sorption paths are needed in optimizing the process variables related to drying, storage, handling and dehulling of agricultural seeds. Much data on moisture sorption behavior of many foods including cereals and oilseeds (Iglesias and Chirife 1982) as well as various theoretical and empirical sorption models (with limitations for each) about their applicability on the nature of foods (Rockland and Stewart 1981) are available. Recently EMC-ERH relationships for some cucurbita seeds such as pumpkin and its fractions (Akritidis *et al.* 1988) and melon seeds (Ezeike 1988) have been discussed. However, no study in this area has been undertaken so far on *karingda* seed and its fractions.

The objectives of this study were to assess the sorption behavior of *karingda* seeds, kernels and hulls at five temperatures and to quantify such behavior using

some established sorption models those have been reported to be in good fit to many cereals and oilseeds. Additionally, a relevant thermodynamic parameter, i.e., the excess heats of sorption of all the three materials have been estimated from the sorption data, and their correlation with the moisture contents of the respective sample has been discussed.

MATERIALS AND METHODS

About one kilogram of karingda seeds was extracted from freshly harvested matured fruits of the Rabi season crop. The initial moisture content of seeds was estimated to be around 35.5% d.b. using an oven drying method (ISI 1966). The seeds were packed in a polythelene bag and kept in a refrigerator at around 4C for subsequent uses. About 100 g of these high moisture seeds (approximately 1200 in number) were taken out from the refrigerator at a time. Fifty grams of these seeds were manually dehulled to obtain the kernels (approximately 35 g) and hulls. The seeds along with kernels and hulls were taken for desorption study. The moisture contents of the kernels and hulls were estimated to be 32.5 and 37.5% d.b., respectively. Part of these freshly harvested seeds (about 500 g) was dried under the sun for 3 to 4 days to bring down the moisture content to around 7.5% d.b. The moisture contents of the corresponding kernels and hulls were determined to be 5.8 and 10.2% d.b. These dried seed, kernel and hull were taken for the adsorption study.

A static gravimetric technique based on isopiestic transfer of water vapor (Glasstone 1968) was used for determination of the equilibrium moisture content of karingda seed and its fraction for adsorption and desorption processes. Saturated solutions of various inorganic salts were employed (Greenspan 1977) to generate the controlled humidity environment in a closed chamber ranging between 11 and 96% (9 levels). Studies of adsorption and desorption processes were carried out at five temperature levels, namely 10, 20, 30, 40 and 50C. The change of equilibrium relative humidity of the salt solutions due to the change in temperature were estimated using the relations reported by Labuza *et al.* (1985).

Nine desiccators were used for this study. Each desiccator was provided with a perforated and raised platform on which to place three small glass weighing bottles. The level of the saturated salt solutions in each desiccator was such that it was below the perforated platform in order to avoid contact of the salt solution and the weighing bottles. For each temperature-humidity condition, about 2-3 g of karingda seed, kernel and hull were put into respective weighing bottles, weighed and kept inside the desiccator. The desiccator lid was provided with an outlet pipe fitted with a stopcock arrangement. Partial vacuum was created inside each desiccator to accelerate the adsorption or desorption of water vapor to and from the sample (Das and Chatteraj 1984; Moreyra and Peleg

1981). All these desiccators were put in a controlled temperature oven (fluctuation within $\pm 1\text{C}$ over the set value), and the gain or loss in weights of the samples in each desiccator was monitored periodically until two consecutive readings were same. This took about 20-27 days, depending upon the nature and initial moisture content of the samples. Each observation was replicated three times and average values of EMC have been reported.

Samples placed in the high humidity environment, e.g., relative humidity greater than 85%, became visibly infected with fungus within 10-12 days of incubation. To minimize or avoid such a phenomenon, seeds, kernels and hulls were treated under UV light for half an hour and then put into previously sterilized weighing bottles. This technique was found to retard the fungus growth considerably.

Four sorption isotherm models were used for the analysis of ERH-EMC data for karingda seed, kernel and hull (Table 1). Models 1-3 are reported to be a better fit for correlating these two parameters at different temperatures for many cereal grains (Rizvi 1986) and oil seeds (Akritidis *et al.* 1988; Mazza and Jayas 1991). The three parameters GAB equation (Model 4), which is fundamentally a refined extension of Langmuir and BET equations, has been suggested to be the most versatile sorption model for fitting these two variables (EMC and ERH) for many foods (Bizot 1983; Van den Berg 1984). Some workers (Labuza *et al.* 1985; Rizvi 1986; Tsami *et al.* 1990; Sopade and Ajisegiri 1994) have reported temperature dependence of the coefficients of the GAB sorption model. The coefficients of the individual equations have been computed by means of a standard regression technique (Snedecor and Cochran 1967). The models have been computed for their suitability in predicting EMC of the sample on the basis of standard error of estimate, mean percent of error and residual plot.

An important thermodynamic parameter usually obtained from sorption data is the excess heat of sorption which provides useful information on the energetics of water sorption processes in food (Rizvi 1986). The excess heat of sorption, (Q_{st}) which is greater than the latent heat of vaporization of pure water at a particular temperature, can be considered as an indication of intermolecular forces between the sorbate and the sorption sites. The trend of Q_{st} with the change in moisture content of the sample gives an idea of availability of polar sites to water vapor as sorption proceeds (Chung and Pfof 1967). Various workers (Labuza 1968; Iglesias and Chirife 1976) have shown that a prediction of water activity (or ERH) of foods at a particular moisture content but at various temperatures can be obtained by applying the Clausius-Clapeyron equation if the value of Q_{st} of the food at that moisture content is known. The values of Q_{st} at different moisture contents could be obtained from the following equation.

$$\ln \left[\frac{\text{ERH}}{100} \right] = \ln(a_w) = \left[- \frac{Q_{st}}{RT_{ab}} \right] + C_i \quad (1)$$

Where, Q_{st} is the excess heat of sorption, J/mole; R is the universal gas constant (8.32 J/mole K); T_{ab} is absolute temperature in K; and C_i is a constant of integration. Q_{st} is the slope of a plot of $\ln(a_w)$ vs $1/T_{ab}$.

TABLE 1.
MOISTURE SORPTION ISOTHERM MODELS USED TO ANALYZE EMC-ERH
DATA FOR KARINGDA SEED, KERNEL AND HULL

Modified-Henderson equation (Henderson 1952; Thompson *et al.* 1968):

$$1 - \text{RH} = \exp \left[- A (T + C) M^B \right] \quad \dots (1)$$

Modified Chung-Pfost equation (Pfost *et al.* 1976) :

$$\text{RH} = \exp \left[\frac{- A}{T + C} \exp \left(- \frac{BM}{100} \right) \right] \quad \dots (2)$$

Modified Halsey equation (Halsey 1948; Iglesias and Chirife 1976):

$$\text{RH} = \exp \left[- \exp (A + B T) M^{-C} \right] \quad \dots (3)$$

Guggenheim-Anderson-de Boer (GAB) equation (Bizot 1983; Van den Berg 1984; Rizvi 1986; Tsami *et al.* 1990; Sopade and Ajisegiri 1994):

$$M / M_o = \frac{C_g K a_w}{(1 - K a_w) (1 - K a_w + C_g K a_w)} \quad \dots (4)$$

$$\text{Where, } M_o = M'_o \exp (E_a / R T_{ab}) \quad \dots (4a)$$

$$C_g = C_o \exp (\Delta H_c / R T_{ab}) \quad \dots (4b)$$

$$K = K_o \exp (\Delta H_k / R T_{ab}) \quad \dots (4c)$$

RESULTS AND DISCUSSION

The mean values of the equilibrium moisture content (EMC) of karingda seed, kernel and hull, measured at different temperatures and relative humidities, are presented in Tables 2 and 3 for adsorption and desorption, respectively.

TABLE 2.
EQUILIBRIUM MOISTURE CONTENT (EMC), % (d.b.) OF KARINGDA SEED,
KERNEL AND HULL DURING THE PROCESS OF ADSORPTION

Temperature, °C									
10		20		30		40		50	
ERH	EMC	ERH	EMC	ERH	EMC	ERH	EMC	ERH	EMC
Seed									
11.3	3.74	11.3	3.44	11.3	2.82	11.1	2.35	11.1	1.79
23.4	5.05	23.1	4.65	21.6	4.06	22.8	3.33	20.4	2.76
33.5	6.47	33.1	6.02	32.4	5.28	31.6	4.31	30.5	3.73
43.5	7.74	43.2	7.17	43.2	6.19	42.0	5.43	41.4	5.01
57.9	9.78	54.4	8.45	51.4	7.12	48.9	6.30	48.4	5.64
72.1	11.31	69.9	10.46	69.7	9.84	66.1	8.56	64.5	7.22
75.5	12.04	75.5	11.64	75.1	10.29	74.7	9.81	74.4	8.84
86.8	14.52	85.1	13.25	83.6	12.27	82.3	11.43	81.2	10.16
96.3	18.74	94.6	16.02	89.1	13.83	85.4	12.19	84.8	11.56
Kernel									
11.3	2.85	11.3	2.25	11.3	2.17	11.1	1.87	11.1	1.21
23.4	4.06	23.1	3.41	21.6	3.39	22.8	2.68	20.4	2.14
33.5	4.88	33.1	4.07	32.4	4.00	31.6	3.20	30.5	2.74
43.5	5.77	43.2	5.17	43.2	4.87	42.0	3.95	41.4	3.65
57.9	7.04	54.4	6.27	51.4	5.28	48.9	4.57	48.4	3.95
72.1	8.12	69.9	7.48	69.7	6.86	66.1	5.74	64.5	5.44
75.5	8.54	75.5	8.41	75.1	7.22	74.7	6.50	74.4	6.12
86.8	10.11	85.1	9.64	83.6	8.44	82.3	7.24	81.2	6.82
96.3	12.15	94.6	11.55	89.1	10.26	85.4	7.94	84.8	7.39
Hull									
11.3	5.12	11.3	3.83	11.3	3.08	11.1	2.58	11.1	2.02
23.4	7.25	23.1	5.25	21.6	4.92	22.8	4.04	20.4	3.42
33.5	8.43	33.1	6.51	32.4	5.96	31.6	5.19	30.5	4.54
43.5	9.87	43.2	7.95	43.2	7.45	42.0	6.15	41.4	5.62
57.9	12.04	54.4	9.56	51.4	8.34	48.9	7.12	48.4	6.49
72.1	14.58	69.9	11.80	69.7	11.32	66.1	9.45	64.5	8.54
75.5	15.74	75.5	12.85	75.1	12.13	74.7	10.95	74.4	10.51
86.8	18.64	85.1	14.85	83.6	14.21	82.3	13.72	81.2	13.11
96.3	21.93	94.6	18.43	89.1	16.85	85.4	15.92	84.8	15.14

Average of three replicates

TABLE 3.
EQUILIBRIUM MOISTURE CONTENT (EMC), % (d.b.) OF KARINGDA SEED, KERNEL
AND HULL DURING THE PROCESS OF DESORPTION

Temperature, °C									
10		20		30		40		50	
ERH	EMC	ERH	EMC	ERH	EMC	ERH	EMC	ERH	EMC
Seed									
11.3	4.39	11.3	4.05	11.3	3.47	11.1	2.88	11.1	2.26
23.4	6.42	23.1	5.69	21.6	5.02	22.8	4.52	20.4	3.48
33.5	7.67	33.1	7.39	32.4	6.84	31.6	5.54	30.5	4.62
43.5	9.34	43.2	8.51	43.2	7.94	42.0	6.66	41.4	5.59
57.9	11.39	54.4	10.13	51.4	9.25	48.9	7.82	48.4	6.36
72.1	13.72	69.9	12.89	69.7	11.92	66.1	10.05	64.5	8.42
75.5	14.65	75.5	14.01	75.1	13.20	74.7	11.54	74.4	9.86
86.8	17.84	85.1	16.22	83.6	15.22	82.3	13.34	81.2	11.38
96.3	21.12	94.6	20.19	89.1	17.24	85.4	14.52	84.8	12.26
Kernel									
11.3	3.16	11.3	3.13	11.3	2.58	11.1	2.17	11.1	1.45
23.4	4.58	23.1	4.33	21.6	3.70	22.8	3.09	20.4	2.36
33.5	5.86	33.1	5.61	32.4	4.46	31.6	3.73	30.5	3.14
43.5	6.95	43.2	6.65	43.2	5.54	42.0	4.73	41.4	4.35
57.9	8.18	54.4	7.97	51.4	5.94	48.9	5.47	48.4	4.90
72.1	9.98	69.9	9.72	69.7	7.82	66.1	6.95	64.5	6.21
75.5	10.75	75.5	10.61	75.1	8.32	74.7	7.93	74.4	7.33
86.8	13.07	85.1	12.38	83.6	9.94	82.3	8.52	81.2	8.07
96.3	16.26	94.6	15.43	89.1	10.98	85.4	8.98	84.8	8.91
Hull									
11.3	5.89	11.3	4.69	11.3	4.08	11.1	3.58	11.1	2.97
23.4	7.96	23.1	6.97	21.6	6.35	22.8	5.36	20.4	4.89
33.5	9.12	33.1	8.56	32.4	8.09	31.6	6.74	30.5	6.36
43.5	10.46	43.2	9.83	43.2	9.42	42.0	7.84	41.4	7.42
57.9	12.67	54.4	11.86	51.4	10.86	48.9	8.94	48.4	8.28
72.1	15.34	69.9	14.65	69.7	13.52	66.1	11.32	64.5	10.84
75.5	16.68	75.5	15.47	75.1	14.76	74.7	13.50	74.4	13.04
86.8	19.49	85.1	17.93	83.6	17.94	82.3	16.25	81.2	15.77
96.3	24.25	94.6	23.40	89.1	21.56	85.4	19.10	84.8	17.70

Average of three replicates

Figure 1 illustrates a typical adsorption isotherm for the karingda seed; the trends for all other isotherms are quite similar (not shown). All isotherms are sigmoid and belong to the type II according to the classification of Brunauer *et*

al. (1940). It is observed that the effect of temperature on EMC is as might be expected for all these samples, i.e., the quantity of moisture sorbed at any particular equilibrium relative humidity (ERH) decreases with the increase in environmental temperature (Iglesias and Chirfie 1982). Comparing a particular relative humidity and temperature, the EMC values for hull were found to be highest for both desorption and adsorption processes which was followed by those of seed and kernel. The difference in sorptive capacity of the materials investigated should be due primarily to the difference in the availability of polar sites (Chung and Pfof 1967). Porous structure of hull and its high cellulose content might have contributed greater capillary forces and a larger number of active sorption sites (Labuza 1975) that lead to higher EMC values. This hierarchy in water sorption similar to other seeds, its kernel and hull, namely pumpkin (Akritidis *et al.* 1988) and sunflower (Mazza and Jayas 1991). Similar to pumpkin seed (Akritidis *et al.* 1988) and other cereal grains (Chung and Pfof 1967; Iglesias and Chirife 1982; Sopade and Ajisehiri 1994), karingda seed, kernel and hull exhibited hysteresis effect at all the temperatures and ERH values; the EMC values are higher in the desorption process compared to those in adsorption process. Figure 2 shows the typical hysteresis effect for karingda seed at 10C.

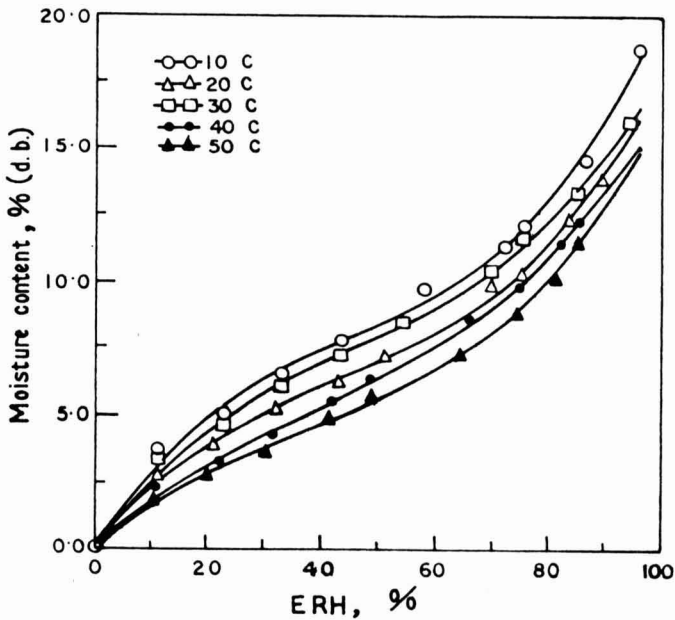


FIG. 1. A TYPICAL ADSORPTION ISOTHERMS OF KARINGDA SEED

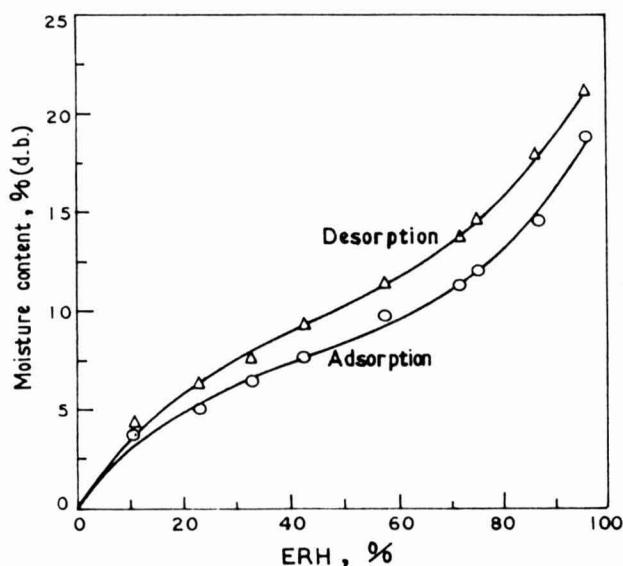


FIG. 2. ADSORPTION-DESORPTION ISOTHERMS OF KARINGDA SEED AT 10C SHOWING HYSTERESIS EFFECT

The coefficients of the Henderson, Chung-Pfost, Halsey and GAB equations (models 1-4 in Table 1) along with individual standard error of estimate (SE) on EMC, mean relative percent error (P) and trend of residual plots are summarized in Tables 4a and 4b. From these tables it is observed that, the standard error of estimate as well as mean relative percent error for seed, kernel and hull were lowest with the GAB equation followed by those of the Chung-Pfost equation for both adsorption and desorption processes. The trend of residual plots with respect to either ERH or temperature was found to be random in nature for both these sorption models as shown in Figs. 3a and 3b. Besides high values of standard error of estimates and mean relative percent error for the Henderson and Halsey equations, the plot of residuals was also found to follow particular trends (not shown). Thus, it suggests that, the sorption behavior of karingda seed, kernel and hull could be explained better using either the Chung-Pfost or the GAB sorption model. Figure 4 illustrates the deviation between the observed and predicted values on EMC for seed and its fraction at 30C in the entire range of ERH using four sorption models. Although, the level of such deviation could not be generalized for all the temperatures and the sorption processes, but it may be that the GAB model gives a very close estimate of EMC of karingda seed, kernel and hull; similar to many foods as reported by others (Labuza *et al.* 1985; Mazza and Jayas 1991; Sopade and Ajisegiri 1994).

TABLE 4a.
THE COEFFICIENTS OF MODIFIED HENDERSON, MODIFIED CHUNG-PFOST AND
MODIFIED HALSEY MODELS FOR KARINGDA SEED, KERNEL AND HULL FOR
ADSORPTION AND DESORPTION PROCESSES

Coefficients	Seeds			Kernel			Hull		
	Hender- son	Chung- Pfof	Halsey	Hender- son	Chung- Pfof	Halsey	Hender- son	Chung- Pfof	Halsey
Adsorption									
A	9.9934x10 ⁻⁴	286.4509	4.9797	12.9220x10 ⁻⁴	321.0273	4.4135	8.4520x10 ⁻⁴	178.4121	5.9190
B	1.8042	21.8977	-0.0626	1.9647	40.7956	-0.0580	1.8262	21.8977	-0.0823
C	-5.9134	35.4509	1.8805	-4.2049	30.7384	1.9958	-8.01254	12.3907	1.8827
SE	3.8180	1.9809	3.6777	0.7222	0.3645	2.1457	8.2183	0.8432	6.0627
P	31.9300	20.2172	22.5987	9.7821	5.3365	18.7369	47.8954	7.5066	30.6867
Residual plot	patterned	random	patterned	patterned	random	patterned	patterned	random	patterned
Desorption									
A	5.8470x10 ⁻⁴	493.0966	5.3397	10.0460x10 ⁻⁴	416.1811	4.6995	3.4800x10 ⁻⁴	241.2603	6.4206
B	1.8543	18.9330	-0.0604	1.9113	33.2418	-0.0576	1.9418	18.9330	-0.0776
C	-4.4337	76.3905	1.9154	-4.6834	53.9953	1.9570	-4.05114	21.6867	2.0025
SE	3.4972	2.0727	3.9262	2.4268	0.6908	2.5406	4.7847	0.9944	6.2097
P	25.1113	18.3791	20.2950	21.1520	7.8185	18.2552	26.3105	6.6816	30.4212
Residual plot	patterned	random	patterned	patterned	random	patterned	patterned	random	patterned

Figure 5 shows the variation of Q_{st} for karingda seed, kernel and hull with moisture content for adsorption and desorption processes. These trends for adsorption and desorption heat of sorption are similar to many cereal grains (Chung and Pfof 1967; Sopade and Ajisegiri 1994; Muthu and Chattopadhyay 1993; Labuza *et al.* 1985); the values of Q_{st} decreased as the moisture content of the sample increased. For each sample, the excess heat of sorption in the desorption process were higher compared to those of adsorption process for the

TABLE 4b.
THE COEFFICIENTS OF GAB MODEL FOR KARINGDA SEED, KERNEL AND
HULL FOR ADSORPTION AND DESORPTION PROCESSES

Parameters	Seed	Kernel	Hull
Adsorption			
M'_O	0.2469	0.6156	0.0762
E_a	7721.21	4792.19	10983.63
C_O	0.0426	0.0232	0.0125
ΔH_c	13690.66	15446.58	17048.69
K_O	1.7008	0.5169	4.2768
ΔH_k	-2174.11	602.76	-4424.71
SE	0.3669	0.2566	1.6937
P	3.3782	3.9893	5.1576
Residual plot	random	random	random
Desorption			
M'_O	0.2310	1.2879	0.5004
E_a	8397.97	3375.48	6679.47
C_O	0.2116	0.0087	0.0201
ΔH_c	9819.67	17836.02	16518.26
K_O	1.1911	0.2230	2.1961
ΔH_k	-1336.89	2756.09	-2756.92
SE	0.4484	0.4698	0.7132
P	3.9514	5.0415	4.0655
Residual plot	random	random	random

entire moisture range considered for computation. This might be attributed to more structural modification in the substance during the desorption process (Iglesias and Chirife 1976). Further, the energies involved to desorb or adsorb water vapor for the hull were more compared to those of kernel and whole seed. It has also been found that the variation of Q_{st} with moisture content follows an exponential relationships for all the samples. Table 5 summarizes the results which shows excellent fit in each case.

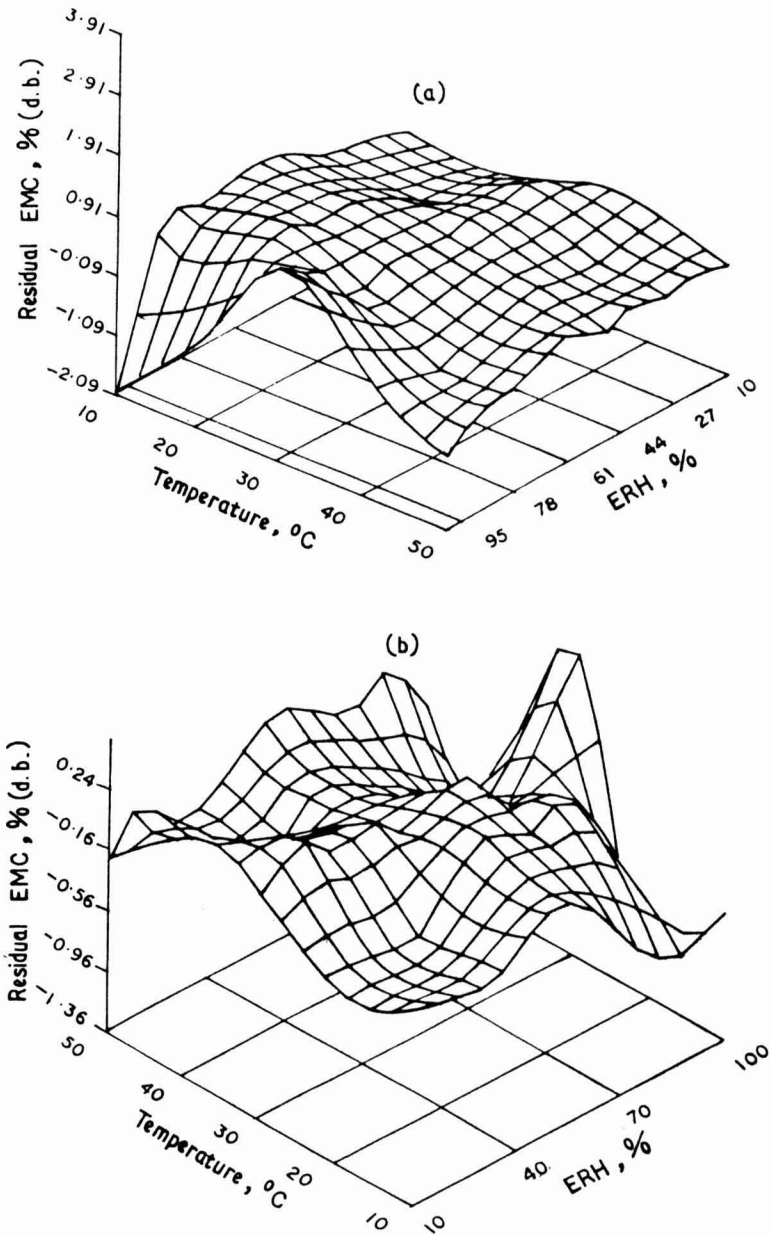


FIG. 3. PLOTS OF RESIDUAL EMC FOR KERNEL OF KARINGDA SEED DURING THE PROCESS OF ADSORPTION AT VARIOUS LEVELS OF ERH AND TEMPERATURE: (a) MODIFIED CHUNG-PFOST MODEL; (b) GAB MODEL

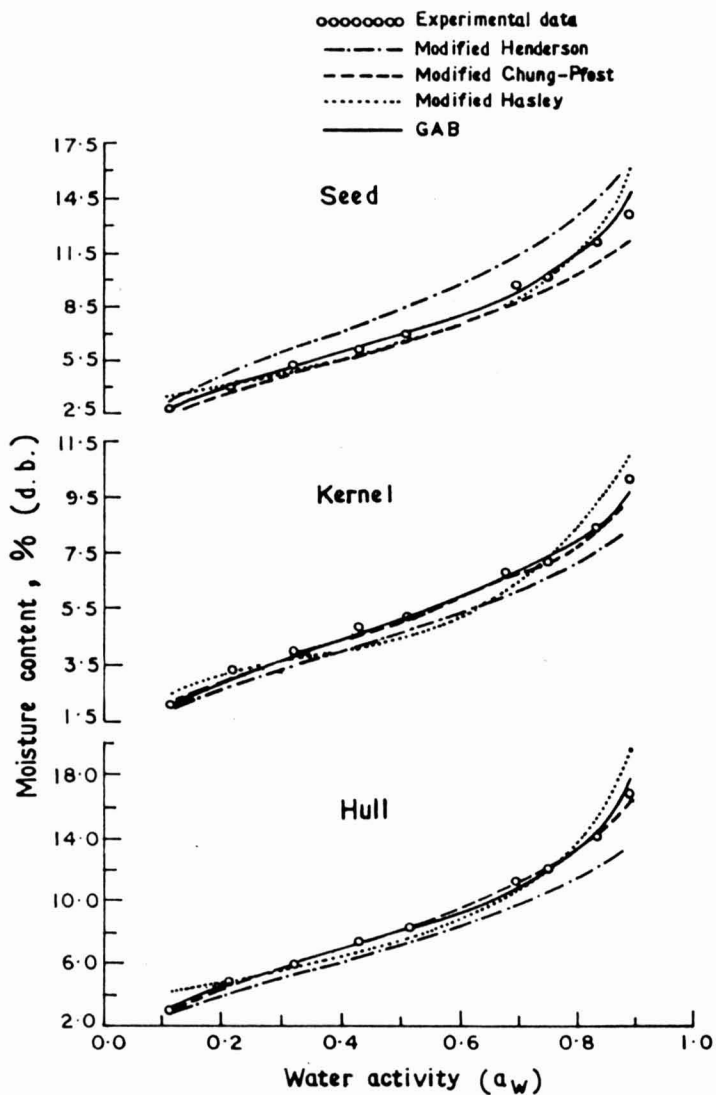


FIG. 4. PREDICTION OF EQUILIBRIUM MOISTURE CONTENT OF KARINGDA SEED, KERNEL AND HULL WITH DIFFERENT SORPTION MODELS FOR ADSORPTION PROCESS AT 30C

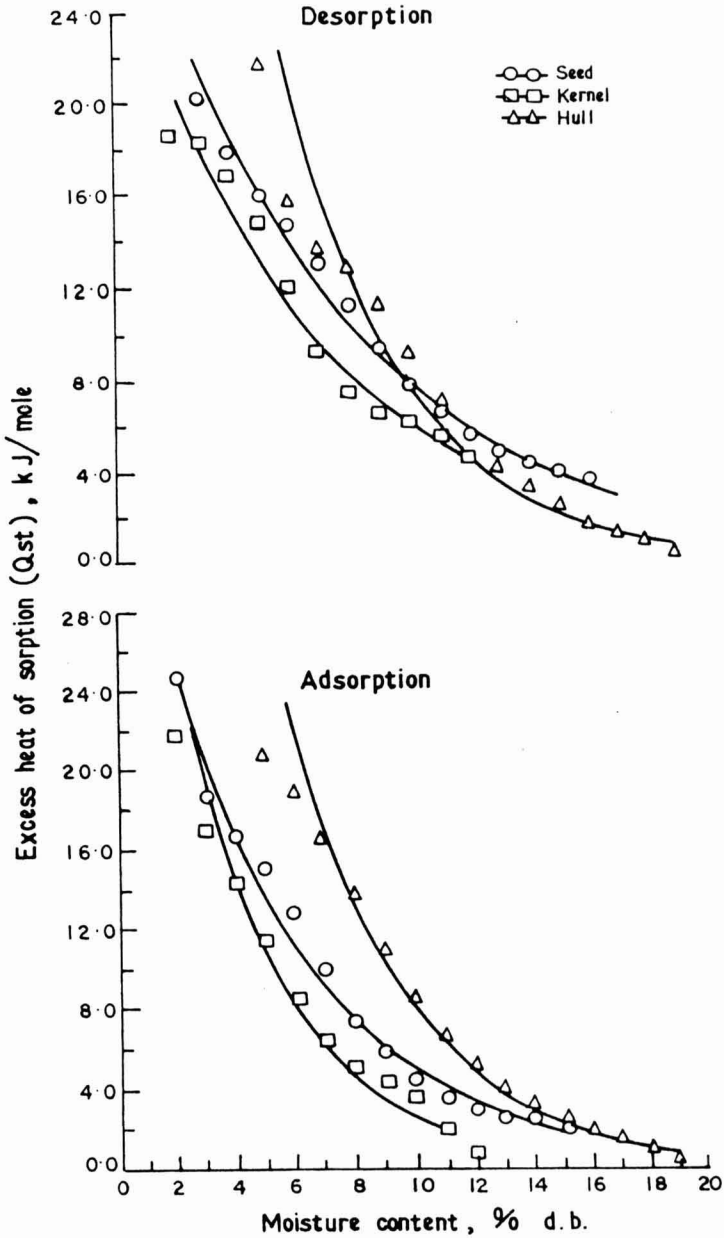


FIG. 5. INFLUENCE OF EQUILIBRIUM MOISTURE CONTENT ON EXCESS HEAT OF SORPTION

TABLE 5.
EXCESS HEAT OF SORPTION - MOISTURE CONTENT RELATIONSHIP
FOR KARINGDA SEED, KERNEL AND HULL

Sample	Equation	Correlation Coefficient
Adsorption		
Seed	$Q_{st} = 8.91 \exp (-0.202 M)$... $r^2 = 0.9854$
Kernel	$Q_{st} = 8.33 \exp (-0.234 M)$... $r^2 = 0.9936$
Hull	$Q_{st} = 22.07 \exp (-0.251 M)$... $r^2 = 0.9667$
Desorption		
Seed	$Q_{st} = 7.83 \exp (-0.143 M)$... $r^2 = 0.9927$
Kernel	$Q_{st} = 6.77 \exp (-0.154 M)$... $r^2 = 0.9728$
Hull	$Q_{st} = 25.31 \exp (-0.265 M)$... $r^2 = 0.9606$

CONCLUSIONS

The trend of moisture sorption isotherms of karingda seed, kernel and hull are sigmoid. For both the adsorption and desorption processes, the equilibrium moisture content of hull at any particular equilibrium relative humidity was highest followed by those of seed and kernel. Among the four sorption models tested namely, the modified Henderson, the modified Halsey, the modified the Chung-Pfost and GAB, the last two models were found to be suitable for describing the sorption behavior of the karingda seed, kernel and hull. Hence, these two models could be employed for the proper management of moisture conditioning of seed or its fraction as required for their processing, handling and storage. The heats of sorption for the seed, kernel and hull, estimated at different moisture contents of the individual samples, showed an exponential relationship between these two variables. The heat of sorption for the hull was

the greatest while that of kernel was the smallest. Such equations relating heat of sorption and moisture content would be very helpful in understanding the energetics involved in the process of hydration (adsorption) and drying (desorption) of karingda seed and kernel.

NOMENCLATURE

A, B, C	Constants for Eq. 1, 2 and 3 (Table 1)
a_w	Water activity, decimal
C_i	Constant of integration for Eq. (1)
C_g	Constant for Eq. 4 (Table 1)
C_o	Constant of GAB equation when the temperature nearing infinity
E_a	Activation energy, J/mole
EMC	Equilibrium moisture content, % d.b.
ERH	Equilibrium relative humidity, %
ΔH_c	Sorption enthalpy associated with the coefficient C_g of Eq. 4 (Table 1), J/mole
ΔH_k	Sorption enthalpy associated with the coefficient K of Eq. 4 (Table 1), J/mole
K	Constant for Eq. 4 (Table 1)
K_o	Constant of GAB equation when the temperature nearing infinity
M	Equilibrium moisture content, % d.b.
M_o'	Monolayer moisture content for Eq. 4 (Table 1), % d.b. when the temperature nearing infinity
P	Mean relative percent error
Q_{st}	Excess heat of sorption, kJ/mole
R	Universal gas constant, 8.32 J/mole K
RH	Equilibrium relative humidity expressed in decimal (a_w) in Eq. (1-3) of Table 1
SE	Standard error estimate on moisture
T	Temperature, °C
T_{ab}	Absolute temperature, K

REFERENCES

- AKRITIDIS, C.B., TSATSARELIS, C.A. and BAGIATIS, C.B. 1988. Equilibrium moisture content of pumpkin seed. *Trans. Am. Soc. Agric. Eng.* 31, 1824-1827.
- BIZOT, H. 1983. Using the "G.A.B." model to construct sorption isotherms. In *Physical Properties of Foods*, (R. Jowitt, F. Eschev, B. Hallstorm, H.F. Th. Meffert, W.E.L. Spiessand and G. Voss, eds.) pp. 43-54, Applied Science Publ., London.

- BRUNAUER, S., DEMING, L.S., DEMING, W.E. and TELLER, D. 1940. On theory of the van der Waals adsorption of gases. *J. Am. Chem. Soc.* 62 1723-1732.
- CHUNG, D.S. and PFOST, H B. 1967. Adsorption and desorption of water vapor by cereal grains and their products. Part II. *Trans. Am. Soc. Agric. Eng.* 10, 549-551.
- DAS, M. and CHATTORAJ, D.K. 1984. Thermodynamics of binding water and solute to myosin. *J. Biosci.* 6, 589-599.
- EZEIKE, G.O.I. 1986. Quasi-static hardness and elastic properties of some tropical seed grains and tomato fruit. *International Agrophys.* 2, 15-29.
- EZEIKE, G.O.I. 1988. Hygroscopic characteristics of unshelled egusi (melon) seeds. *J. Food Sci. Technol.* 23, 511-519.
- GLASSTONE, S. 1968. *Physical Chemistry*. McMillan and Co., London.
- GREENSPAN, L. 1977. Humidity fixed points of binary saturated aqueous solution. *J. Res. for Nat'l. Bureau of Standards - A. Phys. and Chem.* 81A, 89-96.
- HALSEY, G. 1948. Physical adsorption on nonuniform surface. *J. Chem. Phys.* 16, 931-937.
- HENDERSON, S.M. 1952. A basic concept of equilibrium moisture content. *Agric. Eng.* 33, 29-32.
- IGLESIAS, H.A. and CHIRIFE, J. 1976. Prediction of effect of temperature on water sorption isotherms of food materials. *J. Food Technol.* 11, 109-116.
- IGLESIAS, H.A. and CHIRIFE, J. 1982. *Handbook of Food Isotherms: Water Sorption Parameters for Food and Components*. Academic Press, New York.
- I.S.I. 1966. Method of analysis for food grains. Part-II. Moisture. (IS: 4333). Indian Standards Institution, New Delhi.
- JOSHI, A. 1990. Chemical composition and nutritional evaluation of pumpkin, watermelon and karingda seed oil. Unpublished M.Sc. thesis. Department of Food Science, S. P. University, Anand, India.
- JOSHI, D.C. 1993. Mechanical dehulling and oil expression of pumpkin seed. Unpublished Ph. D. thesis. Department of Agricultural and Food Engineering, Post Harvest Technology Centre, Indian Institute of Technology, Kharagpur, India.
- LABUZA, T.P. 1968. Sorption phenomena in food. *Food Technol.* 22, 15-24.
- LABUZA, T.P. 1975. Sorption phenomena in foods: Theoretical and practical aspects. In *Theory, Determination and Control of Physical Properties of Food Materials*, (C. Rha, ed.) pp. 197-219, Reidel Publ. Co., Holland.
- LABUZA, T.P., KANNANE, A. and CHEN, J.Y. 1985. Effect of temperature on the moisture sorption isotherms and water activity shift of two dehydrated foods. *J. Food Sci.* 50, 385-392.

- MAZZA, G. and JAYAS, D.S. 1991. Equilibrium moisture characteristics of sunflower seeds, hulls and kernels. *Trans. Am. Soc. Agric. Eng.* **34**, 534–538.
- MOREYRA, R. and PELEG, M. 1981. Effect of equilibrium water activity on bulk properties of selected food powders. *J. Food. Sci.* **46**, 1918–1922.
- MUTHU, V.P. and CHATTOPADHYAY, P.K. 1993. Prediction of heat of vaporization of moisture from cereal grains-A modelling approach. *Drying Technol.* **11**, 1855–1862.
- PFOST, H.B., MOURER, S.G., CHUNG, D.S. and MILLIKEN, G.A. 1976. Summarizing and reporting equilibrium moisture data for grains. ASAE paper No. 76-3520. St. Joseph, MI:ASAE.
- RIZVI, S.S.H. 1986. Thermodynamic properties of foods in dehydration. In *Engineering Properties of Foods*, (M.A. Rao and S.S.H. Rizvi, eds.) pp. 133–214, Marcel Dekker, New York.
- ROCKLAND, L.B. and STEWART, G.F. (eds.). 1981. *Water Activity: Influence on Food Quality*. Academic Press, New York.
- SINGH, A. 1983. Cultivation of desert melons. *Indian Farming* **8**, 11–13.
- SNEDECOR, G.R. and COCHRAN, W.G. 1967. *Statistical Methods*. Iowa State University Press, Ames, Iowa.
- SOPADE, P.A. and AJISEGIRI, E.S. 1994. Moisture sorption study on Nigerian foods: Maize and Sorghum. *J. Food Process Engineering* **17**, 33–56.
- SUBRAMANIAN, R., SHAMANTHAKA SASTRY, M.C. and VENKATESHMURTHY, K. 1990. Impact dehulling of sunflower seeds: Effect of operating conditions and seed characteristics. *J. Food Eng.* **12**, 83–94.
- TEOTIA, M.S. and RAMAKRISHNA, P. 1984. Chemistry and technology of melon seeds. *J. Food Sci. Technol.* **21**, 332–340.
- THOMPSON, T.L., PEART, R.M. and FOSTER, G.H. 1968. Mathematical simulation of corn drying-a new model. *Trans. Am. Soc. Agric. Eng.* **24**, 582–586.
- TSAMI, E., MARINOS-KOURIS, D. and MAROULIS, Z.B. 1990. Water sorption isotherms of raisins, currants, figs, prunes and apricots. *J. Food Sci.* **55**, 1594–1597, 1625.
- VAN DEN BERG, C. 1984. Description of water activity of foods for engineering purposes by means of the G.A.B. model of sorption. In *Engineering and Food Vol. 1*, (B.M. Mckanna, ed.) Elsevier Applied Science Publ., London.

INACTIVATION KINETICS OF *SALMONELLA DUBLIN* BY PULSED ELECTRIC FIELD

ILKAY SENSOY, Q. HOWARD ZHANG¹ and SUDHIR K. SASTRY

*Department of Food Science and Technology
The Ohio State University
Columbus, Ohio 43210*

Accepted for Publication December 2, 1996

ABSTRACT

Microbial inactivation kinetic models are needed to predict treatment dosage in food pasteurization processes. In this study, we determined inactivation kinetic models of Salmonella dublin in skim milk with a co-field flow high voltage pulsed electric field (PEF) treatment system. Electric field strength of 15-40 kV/cm, treatment time of 12-127 μ s, medium temperatures of 10-50C were tested. A new inactivation kinetic model that combines the effect of treatment time to electric field strength or medium temperature was developed.

INTRODUCTION

Application of high electric field causes electrical breakdown of the microbial cell membrane. Electrical breakdown refers to the loss of the semipermeable property of the cell membrane, and the permeation of large molecules due to osmotic processes (Zimmermann 1986). One of the possible mechanisms is the formation of local instabilities in the membrane by electro-mechanical compression and electrical field induced tension which form pores in the membrane (Zimmerman 1986). Applying an electric field to the medium increases the transmembrane potential difference (V_m) and causes the cell membrane to compress when the critical potential difference ($V_c \sim 0.75-1.25$ V) is exceeded (Knorr *et al.* 1994). This transmembrane potential difference causes the formation of pores and increases the semipermeability and conductivity of the membrane (Zimmermann 1986). Cell lysis occurs when this potential difference is much greater than the critical potential difference (Zimmermann 1986). The breakdown potential is different for different microorganisms (Gupta and Murray 1988; Hulsheger *et al.* 1983, Knorr *et al.* 1994; Mertens and Knorr

Author to whom correspondence should be addressed. 2121 Fyffe Road, Columbus, Ohio, 43210, Phone: 614-688-3644, Fax: 614-292-0218, e-mail: zhang.138@osu.edu

1992; Sale and Hamilton 1967; Zimmermann 1986). It does not depend on pH but on medium temperature (Zimmermann 1986). For a given applied electric field, potential difference developed across the membrane differs according to size of the cell. The smaller the cell, the smaller the potential difference developed (Gupta and Murray 1988; Knorr *et al.* 1994; Zimmermann 1986). Sensitivity of cells to electric field application reaches a minimum in the stationary growth phase (Hulsheger *et al.* 1983). Sensitivity of cells depends more on physiological status than type of microorganisms (Hulsheger *et al.* 1983). Membrane properties such as surface properties or elasticity have been suggested as possible causes of differences in sensitivity to the electric field (Knorr *et al.* 1994).

Short duration of high electric field pulses, i.e., pulsed electric field (PEF), are used to inactivate microorganisms in order to reduce electrolysis (Matsumoto *et al.* 1991, Mizuno and Hori 1988) and to minimize temperature rise (Sale and Hamilton 1967, 1968).

The lethal effect of PEF on vegetative cells and yeasts have been commonly acknowledged (Grahl *et al.* 1992; Gupta and Murray 1988; Hulsheger and Niemann 1980; Hulsheger *et al.* 1981, 1983; Jayaram and Margaritis 1992; Matsumoto *et al.* 1991; Mizuno and Hori 1988; Sale and Hamilton 1967, 1968; Zhang *et al.* 1994a,b,c, 1995b). It is concluded that the lethal effect is not due to heating or electrolysis. It is independent of current density but a function of electric field strength and treatment time (Sale and Hamilton 1967, 1968; Zhang *et al.* 1994a,b; Jayaram *et al.* 1992). The effect of electric field strength is more significant than that of the number of pulses (Qin *et al.* 1994; Knorr *et al.* 1994; Gupta and Murray 1988). However, the occurrence or release of gas bubbles in the medium and subsequent arc-over limit the maximum electric field strength that can be applied. The lethal effect is also a function of the suspension medium temperature as is the change of susceptibility of the microorganisms to the pulsed electric field with the change in temperature (Gupta and Murray 1988; Hulsheger *et al.* 1981; Zhang *et al.* 1994b). Reports on dielectric breakdown studies indicate that the critical transmembrane electroporation voltage (~ 1 V) of cell membrane depends on electrical conductivities of the cytoplasm, σ_c , the membrane, σ_m , and the suspending liquid medium, σ_1 (Jayaram *et al.* 1993; Zimmermann 1986). Lowering the conductivity of the liquid medium increases the difference between the conductivities of the medium and the microbial cytoplasm, which weakens the membrane structure due to an increased flow of ionic substances across the membrane (Jayaram *et al.* 1993). This is also supported by the requirement of lower frequency to cause peak dielectrophoretic response in low conductivity media compared to that required in high conductivity media (Jayaram *et al.* 1993).

Liquid food materials are, in general, electrolytic conductors because of the presence of large concentrations of ions as electrical charge carriers. To

generate a high electric field pulse of several kV/cm within a food, a large flux of electrical current must flow through the treatment chamber for a very short time in the order of microseconds. The time between pulses is much longer than the pulse duration time.

Two practical wave forms are exponential decay and square wave forms in the application of PEF. The square wave form is more efficient than the exponential decay wave form in terms of energy usage (Zhang *et al.* 1994c). The square wave does not cause as much increase in temperature as its exponential decay counterpart (Knorr *et al.* 1994; Neumann *et al.* 1989).

There are three main inactivation kinetic models offered for PEF treatment. Similar to thermal inactivation kinetics, first order reaction models were proposed for both electric field strength and treatment time. In addition, two models combine the effect of electric field strength and treatment time. One is offered by Hulsheger *et al.* (1981), the second one is given by Peleg (1995). They differ in predicting survival fraction at higher values.

We studied the inactivation kinetic models of *Salmonella dublin* as related to electric field strength, treatment time and temperature in milk with a continuous flow PEF treatment chamber. We propose a new combination model for predicting treatment dosage.

MATERIALS AND METHODS

Treatment Chamber Design

The treatment chamber, which holds the food materials during processing, consists of two electrodes and insulating materials that hold the electrodes in position and also form an enclosure for the food materials. Prevention of electrical breakdown of the liquid medium is an important parameter in the design of the treatment chamber. Electrical breakdown may occur because of local field enhancement near an electrode, electrical tracking along an insulation surface, and existence of gas bubbles in liquid foods (Qin *et al.* 1994). This is closely related to the electric field distribution in the chamber (Qin *et al.* 1994). Chambers which have uniform electric field distribution along both the electrode surfaces and the gap axis will give uniform PEF treatment (Qin *et al.* 1994). Electrode surfaces should be large compared to the treatment area and gap between the electrodes should be small to have uniform electric field (Qin *et al.* 1994).

For this research, a continuous co-field flow PEF treatment chamber was designed and constructed. Figure 1 illustrates the conceptual design of this co-field flow PEF treatment chamber. The actual treatment volume is the small orifice volume. The special conical shaped electrodes and insulators were designed to eliminate gas deposits within the treatment volume. The volume of

the orifice and the conical regions were designed so that the electrical resistance of the medium would be high enough for a tetrode high voltage switch tube to handle, and the voltage across the orifice, the treatment zone, was almost equal to the supplied voltage. A Cober Electronics Model 2901 field pulse generator was used to supply the electrical pulses.

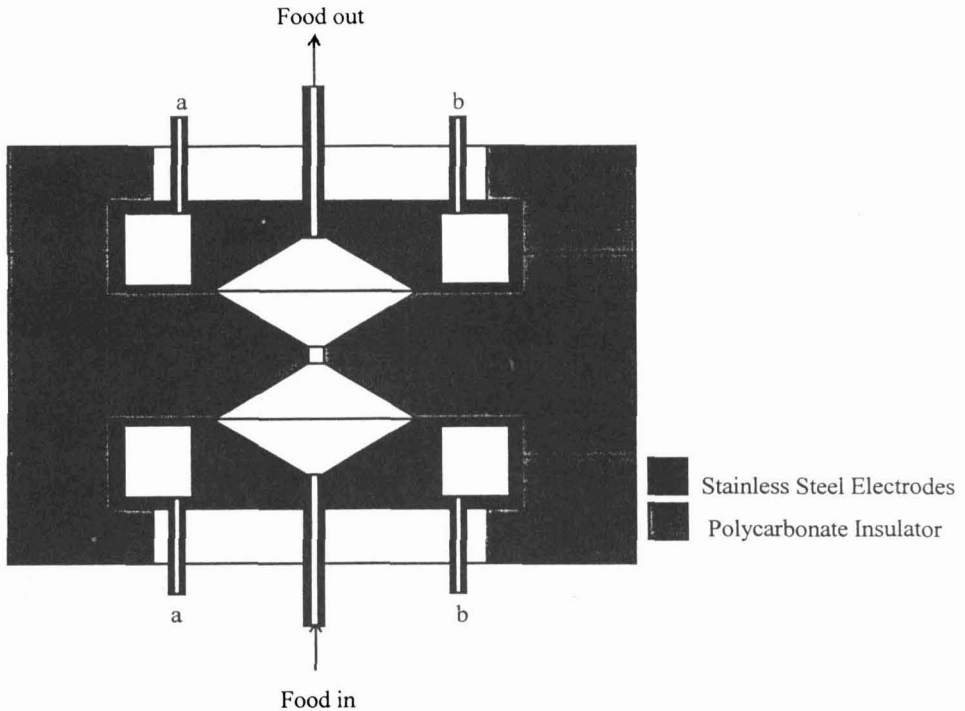


FIG. 1. SIDE VIEW OF THE TREATMENT CHAMBER WHERE "a" COOLING WATER IN AND "b" COOLING WATER OUT FROM THE JACKETS WITHIN THE ELECTRODES

Microbial Analysis

Salmonella dublin (ATCC 15480) was used as an indicator bacterium in skim milk. Freeze dried cultures of *S. dublin* from ATCC were grown and stored in small vials in a freezer according to ATCC procedures. A preculture was prepared by inoculating 0.1 mL from previously frozen cultures to 10 mL sterile nutrient broth and incubating for 12 h at 37°C. The culture was prepared by inoculating 0.1 mL of the preculture to 50 mL sterile nutrient broth and incubating at 37°C. The cultures were harvested at the early stationary phase.

Cells were separated by centrifugation at 3000g for 15 min at 4C. The pellets were re-suspended in 500 mL skim milk to give approximately 10^5 cfu/mL viable cell density. Inoculated milk samples were treated with the PEF treatment system.

Inactivation Kinetics

Temperature of milk entering the chamber was kept constant by passing it through a temperature control coil immersed in a refrigerated water bath, and circulating refrigerated water through the jackets built in the electrodes. The medium temperature never exceeded 30C except in those tests used for temperature effect determination. Inoculated milk was circulated through the treatment chamber for desired treatment time under selected electric field strength, pulse frequency, pulse duration time and volumetric flow rate. The treatment time was calculated assuming that all the liquid had the same treatment. Samples were taken for microbial counts before and after the treatment. Surface plate count numbers were calculated by using the plates that have the number of microorganisms between 25-250. The inactivation results were analyzed by linear regression analysis.

Effect of medium conductivity was tested by treating microorganisms suspended in solutions with different concentrations of KCl with the same electric field intensity. All other tests were done by using skim milk. The effect of electric field strength was tested by applying different electric field strengths at selected frequency, pulse duration and volumetric flow rate. The inactivation effect of temperature increase due to high voltage was minimized by adjusting the inlet medium temperature. Thus, the arithmetic mean of the inlet and outlet temperature at each electric field strength was kept constant. The effect of treatment time was observed by treating inoculated milk samples at selected electric field strength, frequency, pulse duration and flow rate. The volumetric flow rate was adjusted so that the treatment time per pass was constant for each pulse duration. Thus, inlet and outlet temperatures were the same for those two pulse durations. The effect of temperature was tested at selected electric field strength, pulse repetition frequency, pulse duration and volumetric flow rate. Samples were taken at two different total treatment times, 50 and 100 μ s. The temperature increment per pass was kept less than 1C for temperature effect test.

Kinetic Modeling

For electric field strength effect, survival fractions versus electric field strength data were evaluated for two different models. Calculations were repeated at different total treatment times to show treatment time dependency of the constant factors. Model 1 is a first order equation for electric field strength.

$$\text{Model 1} \quad s = e^{-\frac{E-E_c}{k_e}} \quad (1)$$

where s is survival fraction, E is applied electric field strength (kV/cm), E_c is critical electric field strength (kV/cm), k_e is constant factor (kV/cm).

Model 2 is the equation offered by Peleg (1995). Critical electric field strength, E_c , and constant k_e were given as functions of treatment time.

$$\text{Model 2} \quad s = \frac{1}{1 + e^{\frac{E-E_c}{k_e}}} \quad (2)$$

where;

$$k_e(t) = k_{e_0} e^{k_1 t}$$

$$E_c(t) = E_{c_0} e^{-k_2 t}$$

where s is survival fraction, E is applied electric field strength (kV/cm), E_c is critical electric field strength (kV/cm), k_e , (kV/cm), k_{e_0} (kV/cm), E_{c_0} (kV/cm), k_1 ($1/\mu\text{s}$) and k_2 ($1/\mu\text{s}$) are constant factors.

For treatment time effect, survival fractions versus treatment time data were evaluated for two different models. Calculations were repeated at different electric field strengths to show the electric field strength dependency of the constant factors. Model 3 is a first order kinetic model for treatment time.

$$\text{Model 3} \quad s = e^{-\frac{t-t_c}{k_t}} \quad (3)$$

where s is survival fraction, t is total treatment time (μs), t_c is critical treatment time (μs), k_t is constant factor (μs).

Model 4 is the equation offered by Hulsheger *et al.* (1981).

$$\text{Model 4} \quad s = \left(\frac{t}{t_c} \right)^{\left(-\frac{(E-E_c)}{k'} \right)}$$

where s is survival fraction, t is total treatment time (s), t_c is critical treatment time (s), E is applied electric field strength (kV/cm), E_c is critical electric field strength (kV/cm), k' is constant factor (kV/cm).

Effect of temperature on the first order rate constant was evaluated by using k values at different medium temperatures.

RESULTS AND DISCUSSION

The inactivation rate of microorganisms increases with decreasing conductivity in spite of applying equal input pulse energy as illustrated in Fig. 2. Decreasing medium conductivity increases the difference in conductivity between the microorganism cytoplasm and the medium. This causes additional pressure on the microorganism membrane due to osmotic forces and makes it more sensitive to the PEF treatment.

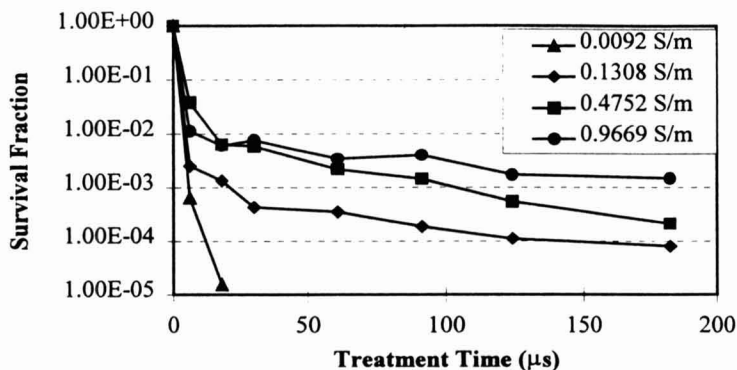


FIG. 2. EFFECT OF CONDUCTIVITY ON SURVIVAL FRACTION VERSUS TIME

Treatment conditions are: electric field strength 28kV/cm, pulse duration 1μs, pulse repetition rate 3.73 kHz.

Both linear and nonlinear kinetic models were evaluated for kinetic study. Electric field strengths of 25 to 40 kV/cm were tested. Increasing the electric field strength increases the inactivation rate logarithmically as illustrated in Fig. 3 and Table 1. Table 1 shows the regression results at different treatment times. For model 1, E_c is the critical electric field strength that gives survival fraction as 1. For model 2, E_c is the electric field that gives the 50 percent survival reduction. For both equations, k_c is the microorganism constant. The two models fit the data well. On the other hand, model 2, second order kinetic equation, also shows bending of the curve at lower electric field strengths. According to data, it can be seen that critical electric field strength, E_c , constants a and k_c are functions of treatment time.

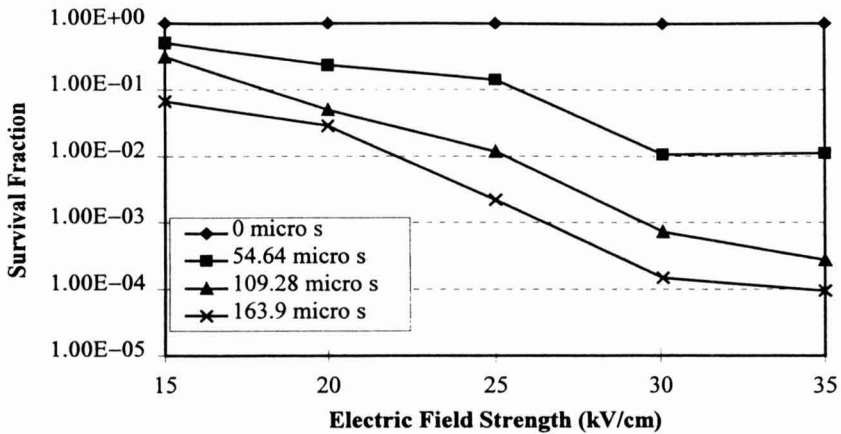


FIG. 3. EFFECT OF ELECTRIC FIELD STRENGTH ON SURVIVAL FRACTION FOR DIFFERENT TREATMENT TIMES

Treatment conditions are: pulse duration 1 μ s, pulse repetition rate 2000 Hz.

Increasing the treatment time decreases the survival fraction logarithmically as seen from Fig. 4. Figure 4 illustrates the treatment time effect at two different pulse duration, 2 and 8 μ s. Regression analyses were performed for 25 to 100 μ s at different electric field strength as tabulated in Table 2. Two kinetic models fit the data, model 3 and 4. For model 3, the data give the critical treatment time t_c as zero. For model 4, t_c is the minimum treatment time that gives s of 1. As observed from Table 2, the constants, k_t and a are functions of electric field strength. This combined equation for electric field and treatment time effect fits the data well. However, Hulsheger *et al.* (1981) obtained this equation by neglecting the data at low electric field strengths and treatment times. The equation is valid where s is lower than 0.5. Another combined

TABLE 1.
MODELS FOR ELECTRIC FIELD STRENGTH EFFECT

Model 1	$S = e^{-\frac{E - E_c}{k_e}}$			
Treatment time		k_e (kV/cm)	E_c (kV/cm)	R^2
25 μ s		7.26	13.76	0.98
50 μ s		3.23	16.21	0.98
75 μ s		2.90	14.92	0.99
100 μ s		2.83	12.56	0.97
		a	t_c (μ s)	R^2
	$e^{\frac{1}{k_e}} = \left(\frac{t}{t_c}\right)^a$	0.16	9.21	0.91
Model 2	$S = \frac{1}{1 + e^{\frac{E - E_c}{k_e}}}$			
Treatment time		k_e (kV/cm)	E_c (kV/cm)	R^2
25 μ s		6.58	16.24	0.98
50 μ s		3.18	16.54	0.98
75 μ s		2.88	15.04	0.99
100 μ s		2.83	12.64	0.97
		k_1 (1/ μ s)	k_{e_0} (kV/cm)	R^2
	$k_e(t) = k_{e_0} e^{k_1 t}$	0.0105	6.98	0.71
		k_2 (1/ μ s)	E_{c_0} (kV/cm)	R^2
	$E_c(t) = E_{c_0} e^{-k_2 t}$	0.0034	18.58	0.80

$\alpha = 0.05$ in all regression analysis

R^2 : Correlation coefficient for regression analysis

equation for treatment time and electric field effect is given by Peleg (1995), as model 2. This equation shows the effect of critical electric field strength as a function of treatment time, which is the case as seen on Table 1. At high electric field strengths both equations give the same fit (Peleg 1995). Another factor that should be considered other than the electric field strength and treatment time is the temperature effect.

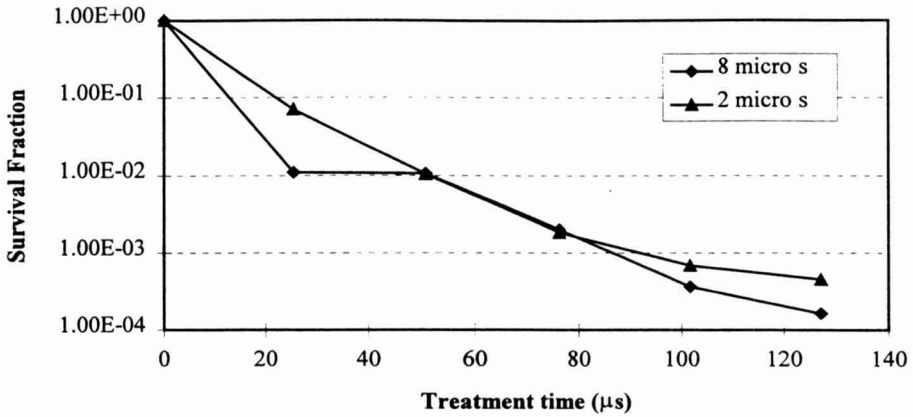


FIG. 4. EFFECT OF TREATMENT TIME ON SURVIVAL FRACTION USING TWO DIFFERENT PULSE DURATION

Treatment conditions are: electric field strength 30 kV/cm, pulse repetition rate 3kHz.

TABLE 2. MODELS FOR TREATMENT TIME EFFECT

Model 3		$s = e^{-\frac{t-t_c}{k_t}}$		
Electric field strength	k_t (µs)	t_c (µs)	R^2	
40 kV/cm	9.20	0	0.92	
35 kV/cm	11.25	0	0.91	
30 kV/cm	13.86	0	0.97	
25 kV/cm	22.30	0	0.87	
$\frac{1}{k_t} = \frac{(E - E_c)}{k_e}$		k_e (kV/cm)	E_c (kV/cm)	R^2
		238.1	13.59	0.99
Model 4		$s = \left(\frac{t}{t_c}\right)^{-a}$		
Electric field strength	a	t_c (µs)	R^2	
40 kV/cm	4.28	10.18	0.99	
35 kV/cm	3.61	10.76	0.96	
30 kV/cm	2.99	11.61	0.98	
25 kV/cm	1.83	11.40	0.99	
$a(E) = \frac{E - E_c}{k_e}$		k_e (kV/cm)	E_c (kV/cm)	R^2
		6.27	12.57	0.98

$\alpha = 0.05$ in all regression analysis

R^2 : Correlation coefficient for regression analysis

There is no model currently proposed for temperature effect in the literature. Temperature effect was tested between the range of 10 to 50C. Increasing the temperature increases the sensitivity of microorganisms to PEF treatment as illustrated in Fig. 5. The regression results at different treatment temperatures are illustrated in Table 3. A new model was developed as Eq. 5, 6 and 7. According to experimental data, there is no critical treatment time as illustrated by model 3. The rate constant, k , first was evaluated as function of electric field strength and then as function of medium temperature as illustrated in Table 3. We verified that temperature effect followed Arrhenius relation. Two first order rate constants in Table 3 should be equal to each other at same treatment conditions. The final survival fraction equation should be in the form:

$$s = e^{-kt} \quad (5)$$

where;

$$k = k_{T_0}(E-E_c) \quad \text{or} \quad (6)$$

$$k = k_{E_0} e^{-\frac{E_A}{RT}} \quad (7)$$

where E is applied electric field strength (kV/cm), E_A is activation energy (J/kg mole), E_c is critical electric field strength (kV/cm), k is survival fraction rate constant ($1/\mu\text{s}$), k_{T_0} ($\text{cm}/\text{kV}\cdot\mu\text{s}$) and k_{E_0} ($1/\mu\text{s}$) are constant factors, R is universal gas constant ($1.9872 \text{ J/kg mole}\cdot\text{K}$), s is survival fraction, and T is medium temperature (K).

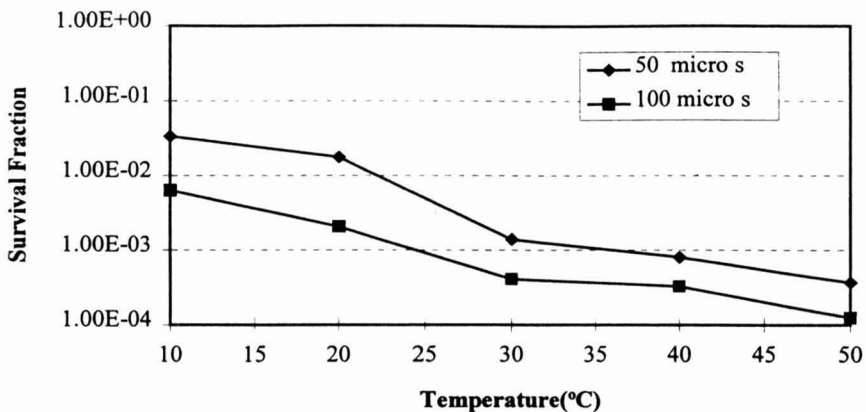


FIG. 5. EFFECT OF TEMPERATURE ON SURVIVAL FRACTION FOR TWO TREATMENT TIMES

Treatment conditions are: electric field strength 25 kV/cm, pulse duration 1 μs , pulse repetition rate 1740 Hz.

TABLE 3.
MODEL FOR SURVIVAL FRACTION AS FUNCTION OF TREATMENT TIME,
ELECTRIC FIELD STRENGTH AND TEMPERATURE

$s = e^{-kt}$		
Electric field strength	$k(1/\mu\text{s})$	R^2
25 kV/cm	0.045	0.87
30 kV/cm	0.072	0.93
35 kV/cm	0.089	0.91
40 kV/cm	0.109	0.92
$k = 0.0042(E - 13.59)$		0.99
Treatment conditions are: $f=2.06$ kHz, $\tau=1\mu\text{s}$, $T=24$ C		
Medium temperature	$k(1/\mu\text{s})$	R^2
283.15 K	0.044	
293.15 K	0.064	
303.15 K	0.059	
313.15 K	0.069	
323.15 K	0.083	
$k = 3.51e^{-\frac{1218.8}{T}}$		0.84
Treatment conditions are: $E=25$ kV/cm, $f=1.7$ kHz, $\tau=1\mu\text{s}$		

$\alpha = 0.5$ in all regression analysis

R^2 : Correlation coefficient for regression analysis

In thermal processing, microbial death kinetics are first order. In the case of PEF processing, the death kinetics also follows the first order kinetics. For temperature effect on the rate constant, the Arrhenius equation was examined. For electric field strength effect model 1 was used. This new equation combines the effect of PEF treatment time to electric field strength or medium temperature. The equation defines the critical electric field strength and shows the strong effect of electric field strength on the inactivation rate. To combine the electric field strength and temperature effect in one equation further study is recommended. Critical electric field strength, E_c , can also be a function of temperature as it is a function of PEF treatment time.

ACKNOWLEDGMENT

Support of this research comes from The Ohio Agricultural Research and Development Center and The US Army Natick Research, Development and Engineering Center. The stipend and the tuition and fees of the first author comes from Kocaeli University, Turkey.

Special thanks go to Dr. Yongguang Yin for operating the PEF treatment system.

NOMENCLATURE

- E Actual peak electric field strength (kV/cm)
- E_A Activation energy (J/kg mole)
- E_c Critical electric field strength (kV/cm)
- E_{c_0} Constant factor (kV/cm)
- k_0 Inactivation rate constant ($1/\mu\text{s}$)
- k' Constant factor (kV/cm)
- k_e Constant factor (kV/cm)
- k_{e_0} Constant factor (kV/cm)
- k_{E_0} Constant factor ($1/\mu\text{s}$)
- k_{T_0} Constant factor ($\text{cm}/\text{kV}\cdot\mu\text{s}$)
- k_t Constant factor (μs)
- k_1 Constant factor ($1/\mu\text{s}$)
- k_2 Constant factor ($1/\mu\text{s}$)
- s Microbial survival fraction (cfu after treatment/ cfu before treatment)
- t Treatment time (μs)
- t_c Critical treatment time (μs)
- T Temperature (K)
- V Peak discharge voltage (kV)
- V_c Critical potential difference (V)
- V_m Transmembrane potential difference (V)
- σ_c Conductivity of the microorganism cytoplasm (S/m)
- σ_1 Conductivity of the microorganism membrane (S/m)
- σ_m Conductivity of the liquid medium (S/m)

REFERENCES

- GRAHL, T., SITZMAN, W. and MARKL, H. 1992. Killing of microorganisms in fluid media by high voltage pulses. DEHEMA Biotechnol. Conference Series. 5B, 675–678.

- GUPTA, R.P. and MURRAY, W. 1988. Pulsed high electric field sterilization. IEEE Pulsed Power Conference Record. pp. 58-64.
- HULSHEGER, H., POTEI, J. and NIEMANN, E.-G. 1980. Lethal effects of high-voltage pulses on *E. coli* K12. *Radiation and Environmental Biophysics* 18, 281-288.
- HULSHEGER, H., POTEI, J. and NIEMANN, E.-G. 1981. Killing of bacteria with electric pulses of high electric field strength. *Radiation and Environmental Biophysics* 20, 53-65.
- HULSHEGER, H., POTEI, J. and NIEMANN, E.-G. 1983. Electric field effects on bacteria and yeast cells. *Radiation and Environmental Biophysics*, 22, 149-162.
- JAYARAM, S., CASTLE, G.S.P. and MARGARITIS, A. 1992. Kinetics of sterilization of *Lactobacillus brevis* cells by the application of high voltage pulses. *Biotechnol. and Bioeng.* 40, 1412-1420.
- JAYARAM, S., CASTLE, G.S.P. and MARGARITIS, A. 1993. The effects of high field DC pulse and liquid medium conductivity on survivability of *Lactobacillus brevis*. *Applied Microbiol. and Biotechnol.* 40, 117-122.
- KNORR, D., GEULEN, M., GRAHL, T. and SITZMANN, W. 1994. Food application of high electric field pulses. *Trends in Food Sci. & Technol.* 5, 71-75.
- MATSUMOTO, Y., SHIOJI, N., SATAKE, T. and SAKUMA, A. 1991. Inactivation of microorganisms by pulsed high voltage application. Conference Record of IEEE Industrial Applications Society Annual Meeting, pp. 652-659.
- MERTENS, B. and KNORR, D. 1992. Development of nonthermal processes for food preservation. *Food Technol. May*, 125-133.
- MIZUNO, A. and HORI, Y. 1988. Destruction of living cells by pulsed high-voltage application. *IEEE Transactions on Industry Appl.* 24 (3), 387-394.
- NEUMANN, E., SOWERS, A.E. and JORDAN, C.A. 1989. *Electroporation and Electrofusion in Cell Biology*. Plenum Press, New York.
- PELEG, M. 1995. A model of microbial survival after exposure to pulsed electric fields. *J. Sci. Food and Agric.* 67, 93-99.
- QIN, B.-L., ZHANG, Q., BARBOSA-CANOVAS, G.V., SWANSON, B.G. and PEDROW, P.D. 1995. Pulsed electric field treatment chamber design for liquid food pasteurization using a finite element method. *Transactions of ASAE.* 38(2), 557-565.
- SALE, A.J.H. and HAMILTON, W.A. 1967. Effects of high electric fields on microorganisms; I. Killing of bacteria and yeasts. *Biochimica et Biophysica Acta* 148, 781-788.

- SALE, A.J.H. and HAMILTON, W.A. 1968. Effects of high electric fields on micro-organisms; III. Lysis of erythrocytes and protoplasts. *Biochimica et Biophysica Acta* 163, 37-43.
- ZHANG, Q., BARBOSA-CANOVAS, G.V. and SWANSON, B.G. 1995a. Engineering aspects of pulsed electric field pasteurization. *J. Food Eng.* 25, 261-281.
- ZHANG, Q., CHANG, F.-J., BARBOSA-CANOVAS, G.V. and SWANSON, B.G. 1994a. Inactivation of microorganisms in a semisolid model food using high voltage pulsed electric fields. *Food Sci. Technol. (Lebensmittel-Wissenschaft und Technologie)* 27(6), 538-543.
- ZHANG, Q., MONSALVE-GONZALEZ, A., BARBOSA-CANOVAS, G.V. and SWANSON, B.G. 1994b. Inactivation of *E. coli* and *S. cerevisiae* by pulsed electric fields under controlled temperature conditions. *Transactions of the ASAE*, 37 (2), 581-587.
- ZHANG, Q., MONSALVE-GONZALEZ, A., QIN, B.-L., BARBOSA-CANOVAS, G.V. and SWANSON, B.G. 1994c. Inactivation of *Saccharomyces Cerevisiae* by square wave and exponential-decay pulsed electric fields. *J. Food Process Engineering* 17(4), 469-478.
- ZHANG, Q., QIN, B.L., BARBOSA-CANOVAS, G.V. and SWANSON, B.G. 1995b. Inactivation of *E. coli* for food pasteurization by high-strength pulsed electric fields. *J. Food Processing and Preservation* 19, 103-118.
- ZIMMERMANN, U. 1986. Electrical breakdown, electroporation and electrofusion. *Reviews of Physiology, Biochemistry, and Pharmacology* 105, 175-256.

TEXTURAL AND VISCOELASTIC CHANGES OF CANNED BISCUIT DOUGH DURING MICROWAVE AND CONVENTIONAL BAKING

B. PAN

*Department of Food Science and Nutrition
University of Missouri, Columbia
Columbia, MO 65211*

AND

M.E. CASTELL-PEREZ¹

*Department of Agricultural Engineering
Texas A&M University
Scoates Hall
College Station, Texas 77843-2117*

Accepted for Publication February 10, 1997

ABSTRACT

Textural changes of canned biscuit wheat dough during microwave and conventional baking were described and contrasted using empirical methods. Drastic increases of specific volume and modulus of elasticity were observed in the beginning and the ending periods of both baking processes. Weight loss showed a significantly ($p < 0.001$) linear relationship with baking time for both baking methods, but the weight loss rate constant for microwave baking was 0.36%/s significantly ($p < 0.01$) higher than conventional baking. Multi-dimensional Scaling showed that microwave baking for 50 s best resembles the textural characteristics of wheat dough under conventional baking for 10 min. Stress relaxation modeling indicated that microwave baking produced higher viscosity and modulus of elasticity values which translates into baked biscuits with undesirable tougher texture.

INTRODUCTION

Microwave heating techniques have many unique advantages when compared to conventional heating methods because they are (1) convenient to operate and control, (2) energy-efficient and (3) clean. These advantages make microwave ovens common household appliances today (Giese 1992). Thus,

¹Corresponding author.

besides trying to adopt these techniques into food processing operations such as drying or pasteurization, the food industry has been developing microwavable products for families and foodservice industry with various degrees of success. However, development of acceptable microwave-baked goods is still a problem because of the less desirable texture, color and aroma of the products. These microwaved bakery products are often described by consumers as flat, with tough and leathery crumbs but without crust and sufficient browning (Shukla 1993).

Wheat dough, the intermediate product in transformation from wheat flour to breads, biscuits, crackers and other bakery foods, is characterized as a viscoelastic material in rheology (Castell-Perez and Steffe 1992; Eliasson 1990). The peculiar viscoelastic properties will not only determine the final product texture but also affect many processing operations such as molding and sheeting (Bloskma 1990a,b).

The change of predominantly viscous wheat dough into predominantly elastic bread during baking/heating may be attributed to: (1) interactions between gluten and gelatinized starches (Dreese *et al.* 1988), (2) interactions between lipids and gelatinized starches (Biliaderis and Tonogai 1991), (3) gluten/protein denaturation (Bale and Muller 1970) and others (starch-starch interactions, etc.). Different heating methods affect these physicochemical changes differently and products usually have different textures (Umbach *et al.* 1992).

This study aims to observe and contrast the textural changes of canned biscuit wheat dough in terms of modulus of elasticity, weight loss and density during microwave and conventional oven baking, and to characterize the viscoelastic changes of wheat dough by modeling its stress relaxation behavior using an empirical approach. Results should aid to the understanding of quality changes (texture) due to the baking treatment for further improvement of microwavable baked goods.

MATERIALS AND METHODS

Preparation of Wheat Dough Samples

Chemically leavened, canned biscuit wheat dough samples (cylindrical shape of 25 mm diameter and 5 mm height, 20 g weight with approximately 60% water content (d.b)) were bought from a local store. Samples were divided into two groups. The first group was baked in a countertop microwave oven (model JE1468L, General Electric Appliances, Louisville, KY) for 10, 20, 30, 40, 50, and 60 s at the full power level (900 watts with 2450 MHz frequency). One biscuit was heated at a time and each sample was placed at a marked point at the center of the oven. Before the baking proceeded, 1 L of water was heated for

3 min to warm up the microwave oven. The second group was baked in a conventional oven (model E36, Vulcan-Hart, Baltimore, MD) at 425F (218.3C) for 2, 4, 6, 8, 10 and 12 min. Raw dough samples without any baking were used as control. A total of 13 treatments with 2 samples each was replicated as a block.

Determination of Texture Indicators

Three characteristics were selected as indicators of the texture of the baked material because they are easy to measure and reveal different aspects of wheat dough structure.

Weight Loss. In this study, weight loss represents mainly water loss, even though carbon dioxide and volatiles are also lost during the heating process. The weight of each dough sample was measured using an electronic balance (Model 610D, Sartorius Instruments Ltd., Edgewood, NY) immediately before and after baking (samples were allowed to cool for 2 min). Weight loss was determined according as:

$$L = ((W_1 - W_2) / W_1) \times 100 \quad (1)$$

where, L is sample weight loss percentage during baking (%)

W_1 is sample weight before baking (g)

W_2 is sample weight after baking (g)

Density. The value of density is a measure of the gas retention capability of the dough and it is inversely related to specific volume, ν , which is an essential texture indicator for dough and baked products set by the American Institute of Baking (Matz 1960). Density was determined according to the formula:

$$\rho = W_2 / V \quad (2)$$

where, ρ is sample density (kg/m³)

V is sample volume (m³),

and $V = \pi h_0 (d/2)^2$, where d is sample diameter (m) and h_0 is sample height before compression (mm). The volume of the samples was calculated by assuming a cylindrical geometry (Finney *et al.* 1949). The height and diameter of each sample after baking (and cooling) were measured using a plastic ruler (means of two readings).

Modulus of Elasticity. After baking and cooling to ambient temperature, the dough samples were compressed to 80 percent of their original height using an Instron Universal Testing Machine (Model 1011, Instron Corp., Canton, MA). Cross-head speed was 100 mm/min. A 50 kg capacity load transducer mounted with a 36 mm diameter aluminum plunger was used. The chart recorder speed was 200 mm/min. The secant modulus of elasticity was used to express the softness or firmness of samples (Instron Corp. 1986). Even though a course indicator, the use of the secant modulus reduces the error caused by differences in sample heights and nonhomogeneity during cooking when compared to force (N) or stress (Pa) as a hardness indicator. Thus,

$$G = \sigma / \gamma \quad (3)$$

where, G is secant modulus of elasticity (Pa)

σ is stress (Pa)

γ is strain

and

$\sigma = F/A$ where F is peak force (N) and A is area of plunger (0.0010179 m²).

Stress Relaxation Tests

Samples baked in the conventional oven for 10 min or in the microwave oven for 50 s were subject to 75 percent constant compressive strain for 1 min by the Instron Universal Testing Machine to determine the force-time curves, which were recorded and later converted into readings for further manipulation and modeling.

Though many stress relaxation models are available, residual analysis as a tool to detect model deficiency has never been performed on these models. In a preliminary study (Pan and Castell-Perez 1994), a series of models were evaluated including Peleg's model (Peleg 1980), Nolan's model (Nolan 1987; Diefes *et al.* 1993), Generalized Maxwell models and others (Peleg and Pollak 1982).

Peleg's Model. This model has been widely used by food scientists and is expressed as

$$t/Y(t) = 1/ab + t/a \quad (4)$$

where, $Y(t)$ is normalized decaying parameter (dimensionless) and

$$Y(t) = 1 - \sigma(t)/\sigma(0)$$

$\sigma(t)$ is stress at time the t th second (kPa)

$\sigma(0)$ is stress at time the 0 th second (kPa)

a is hypothetical asymptotic level of stress not relaxed at infinite time, dimensionless, and $0 \leq a \leq 1$

b is stress decaying rate (1/s)

t is relaxing time (s)

Nolan's Model. This model expresses Peleg's normalized decaying parameter as a power law function of relaxing time:

$$Y(t) = c.t^n \quad (5)$$

where, $Y(t)$ is normalized decaying parameter (dimensionless)

c is fractional loss of the initial compressive force at $t = 1$ s (second⁻ⁿ)

n is rate of relaxation (dimensionless)

t is relaxing time (s)

Other Models. An inverse function model (Pan 1994) and the 5-parameter Wiechert model, were also tested. The inverse function model is simple and its parameters are easy to explain as expressed as

$$\sigma(t)/\gamma_0 = G/(kt + 1) + G_e \quad (6)$$

where, G is relaxing modulus (Pa)

G_e is equilibrium modulus (Pa)

t is relaxing time (s)

k is viscoelastic index or the ratio of viscosity to elasticity (s^{-1}). The smaller the k value, the more elastic or less viscous the material; materials are purely elastic when $k=0$ and purely viscous when $k = \infty$. The 5-parameter arrheo-dictic Wiechert model (or Generalized Maxwell model) was also used as reference because it is a constitutive equation (Tschoegl 1989):

$$\sigma(t)/\gamma_0 = G_e + \sum G_i \cdot \exp(-G_i \cdot t/\mu_i) \quad (i=2) \quad (7)$$

where, $\sigma(t)$ is stress at time the t th second

γ_0 is strain (%), a known constant

G_e is equilibrium modulus (Pa), and $G_e > 0$

G_i is modulus of elasticity (Pa)

μ_i is viscosity (Pa*s)
 t is relaxing time (s)

The equilibrium modulus of the baked dough, G_e , was determined using nonlinear regression procedures (Gauss method). Parameter settings of the Instron were the same as described in the previous section. Specific baking times (10 min for conventional baking and 50 s for microwave baking) were selected based on Multi-Dimensional Scaling analysis (Fig. 1). Parameter estimation and analysis was conducted to determine the difference, if any, between the two baking methods with respect to their effects on the change of the viscoelastic properties of the dough.

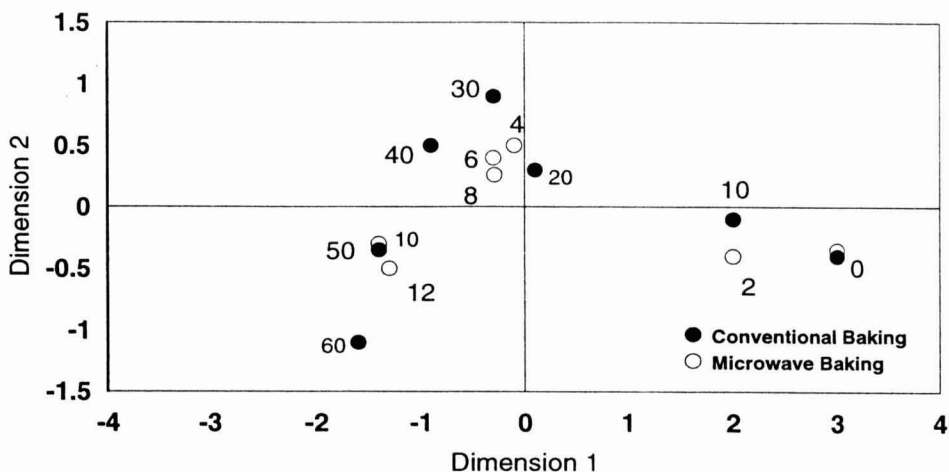


FIG. 1. DERIVED SIMULUS CONFIGURATION EXPRESSING DISSIMILARITIES AMONG DIFFERENT BAKING TREATMENTS BY MULTIDIMENSIONAL SCALING

Experimental Design and Data Analysis

A nested design (heating treatment and time within treatment) was employed. Analysis of variance (ANOVA) and Multivariate analysis of variance (MANOVA) were conducted using the Generalized Linear Models (GLM) procedure of the Statistical Analysis System (SAS 1985). Residual analysis was performed before the outputs were adopted. The Duncan's multiple range test at $p < 0.05$ significant level was used for mean separation where treatment

effects were significant at $p < 0.05$ significant level. Multidimensional scaling (MSD) was performed using the PROXIMITIES and ALSICAL procedures in Statistical Package for the Social Sciences (SPSS 1988).

RESULTS AND DISCUSSION

Changes on Texture Indicators During Baking

The three texture indicators are highly ($p < 0.001$) correlated with each other. The modulus of elasticity and weight loss of wheat dough increased with time while the density decreased with time for both baking methods (Table 1). The following observations were made:

(1) The weight loss of wheat dough during baking showed a linear relationship ($p < 0.001$) with time for both baking methods (Fig. 2). The weight-loss-rate constant for microwave baking, 0.36%/s (or g water/g dough/s), given by the slope of the line, was significantly ($p < 0.001$) higher than that for conventional baking, 0.03%/s.

(2) Density changes of wheat dough during baking can be divided into two phases: (1) an early phase, in which dough density decreased dramatically due to volume increase. Nearly 90% of density reduction occurred in the first 30 s for microwave heating and the first 4 min for conventional heating; and (2) a late phase, in which density decreased slowly due to weight/water loss. The total volume of wheat dough actually changed little at this phase. The existence of the late phase implies that density may not be a good texture indicator at some ranges.

(3) The moduli of elasticity of wheat dough samples subject to microwave baking had much larger standard deviations than those subject to conventional baking. The increase in the modulus of elasticity of wheat dough was nonsignificant ($p < 0.05$) up to the first 40 s of microwave baking, but it increased dramatically during the last 20 s of heating, exceeding the range of acceptable firmness of 50-150 kPa (Matz 1960). A similar change was observed for the wheat dough baked in the conventional oven (after 8 min of heating) but the change was less dramatic. These results indicate that the change on sample firmness due to microwave baking is more sensitive or less robust to changes on baking time than in conventional baking. This is mainly due to the difference in heating methods and it manifests the importance of accurate baking time control for microwave baking operations.

A further overall textural comparison including all of the three studied texture indicators (density, weight loss and modulus of elasticity) using metric Multi-Dimensional Scaling (MDS) analysis suggested that 50 s in microwave

baking would best resemble the textural characteristics of wheat dough baked in conventional oven 10 min (Fig. 1).

TABLE 1.
TEXTURE INDICATORS¹ OF CANNED BISCUIT DOUGH SAMPLES

Baking method and time	modulus of elasticity (kPa)	weight loss (%)	density (kg/m ³)
control	12.85 d	0.00 h	826.42 a
microwave (seconds)			
10	10.58 d	2.03 g	688.48 b
20	19.13 d	6.51 f	425.87 c
30	29.06 d	12.50 d	356.65 cde
40	51.00 cd	14.20 c	305.64 def
50	158.43 b	18.28 b	285.43 fg
60	273.43 a	20.97 a	246.10 g
conventional (minutes)			
2.0	21.90 d	2.78 g	700.27 b
4.0	36.29 d	5.44 f	387.36 cd
6.0	47.34 cd	8.59 e	364.28 cde
8.0	53.74 cd	11.91 d	358.01 cde
10.0	92.86 c	14.56 c	321.76 def
12.0	182.05 b	19.42 b	334.07 def

¹ Means in each column followed by the same letter are not significantly ($p > 0.05$) different ($n \geq 4$).

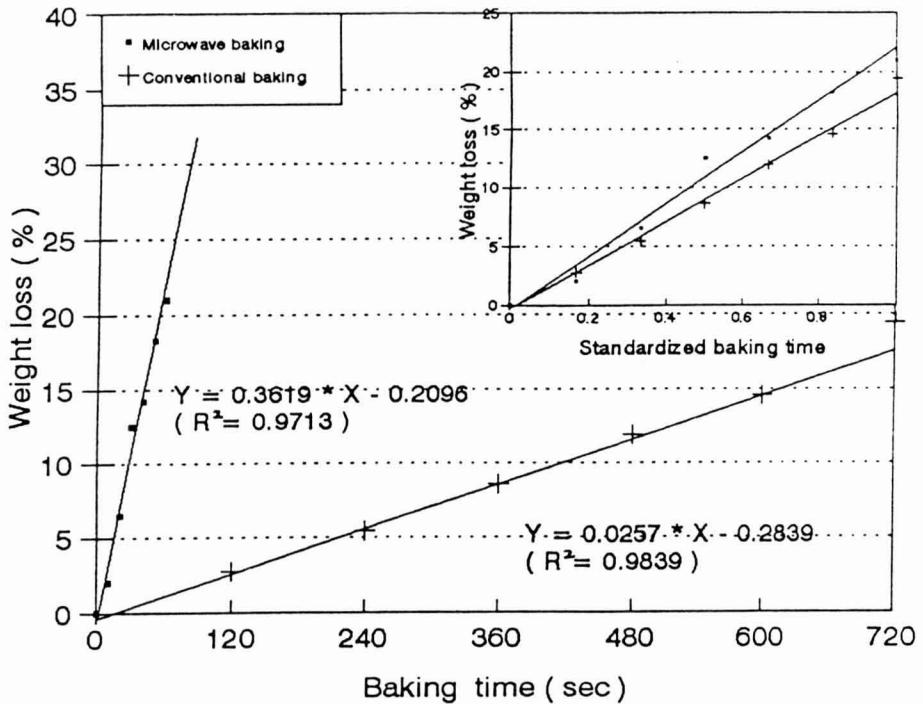


FIG. 2. CHANGE OF WEIGHT LOSS IN CANNED WHEAT DOUGH DURING MICROWAVE AND CONVENTIONAL BAKING

Viscoelastic Analysis of Canned Wheat Dough

Figures 3 and 4 show typical stress relaxation curves and the residual plots for Peleg's and Nolan's models for samples baked in a microwave oven for 50 s. Similar results were observed for the samples baked in the conventional oven.

Peleg's model (Eq. 4) always overestimated $t/Y(t)$ at the middle and underestimated $t/Y(t)$ at the two ends, as shown in the residual plot (Fig. 3). Nolan's model (Eq. 5) always overestimated $Y(t)$ and thus underestimated the equilibrium stress or modulus (Fig. 4).

The inverse function model (Eq. 6) fitted the data very well though it showed some deficiencies in the residual plot (Fig. 5). The 5-parameter Wiechert model (Eq. 7) gave a very good fit and showed a random residual pattern (Fig. 6). Based on goodness of fit and residual analysis, these two models were finally selected for further parameter estimation and comparison of the viscoelastic properties of the baked sample.

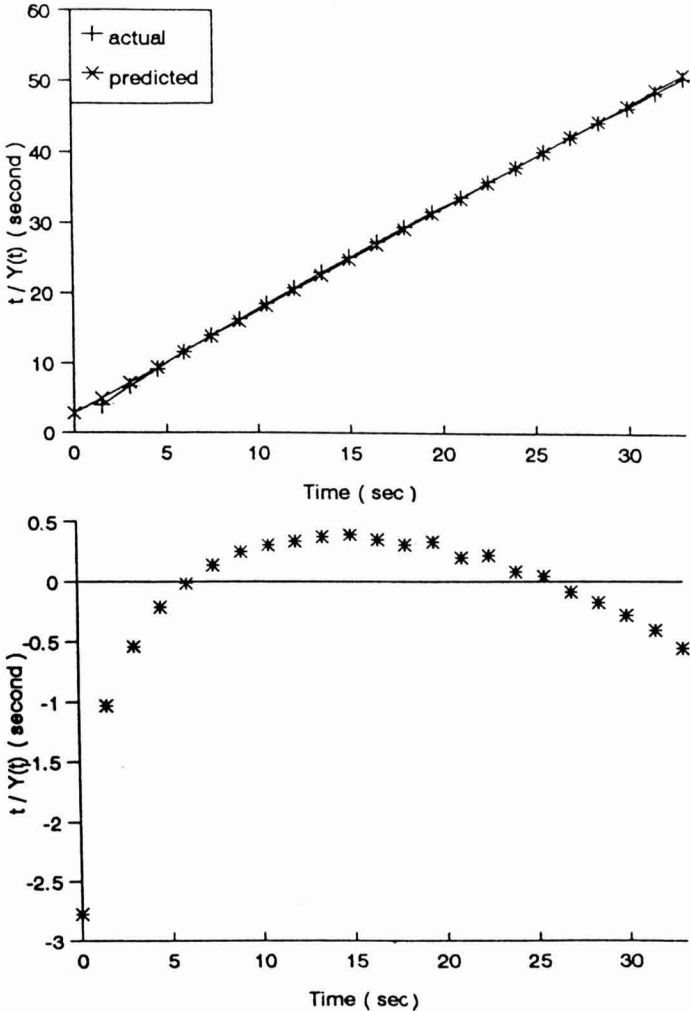


FIG. 3. STRESS RELAXATION CURVE USING PELEG'S MODEL AND ITS RESIDUAL PLOT

Analysis of Viscoelastic Parameters

Analysis of parameters indicates that the equilibrium modulus, G_e , of baked canned wheat dough is significantly ($p < 0.05$) different from zero (arrheodictic viscoelasticity). Differences between the two baking methods with respect to their effects on the viscoelastic properties of wheat dough included two aspects (Table 2):

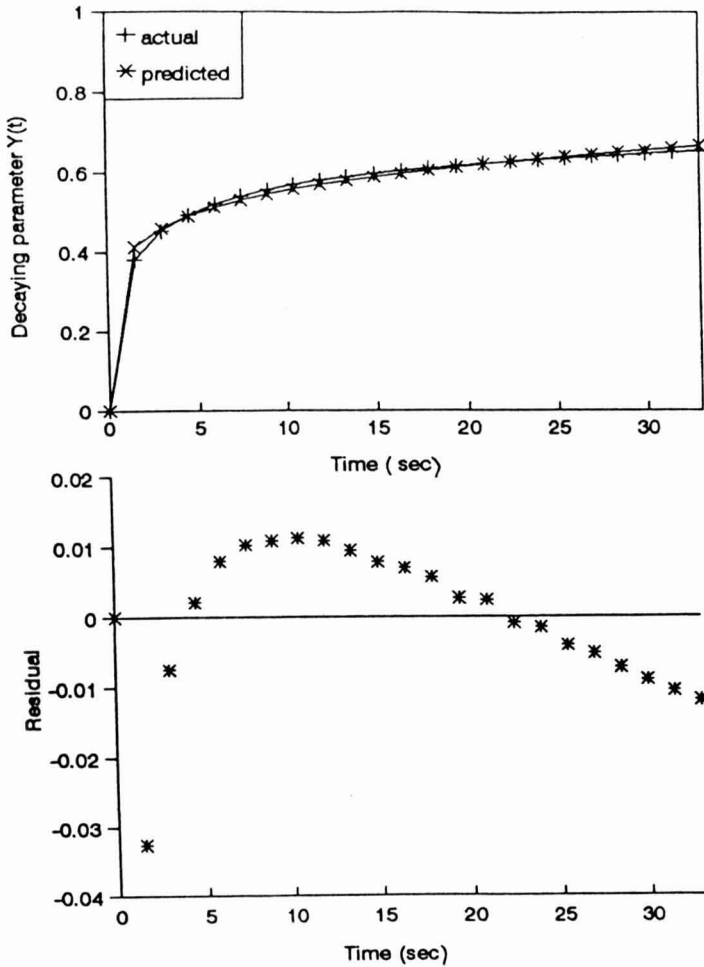


FIG. 4. STRESS RELAXATION CURVE USING NOLAN'S MODEL AND ITS RESIDUAL PLOT

(1) The viscoelastic index, k (Eq. 6), of the wheat dough samples baked in the microwave oven was significantly ($p < 0.05$) higher (0.92) than those baked in the conventional oven (0.69). This seems to indicate that microwave baking produced a product with higher viscous component than conventional baking.

(2) The estimated moduli of elasticity (G_e , G_i) for the canned wheat dough samples baked in the microwave oven were much larger than those baked in the conventional oven. This suggests that the wheat dough samples baked in a microwave oven are more solid-like (more elastic) which relates to harder/firmer

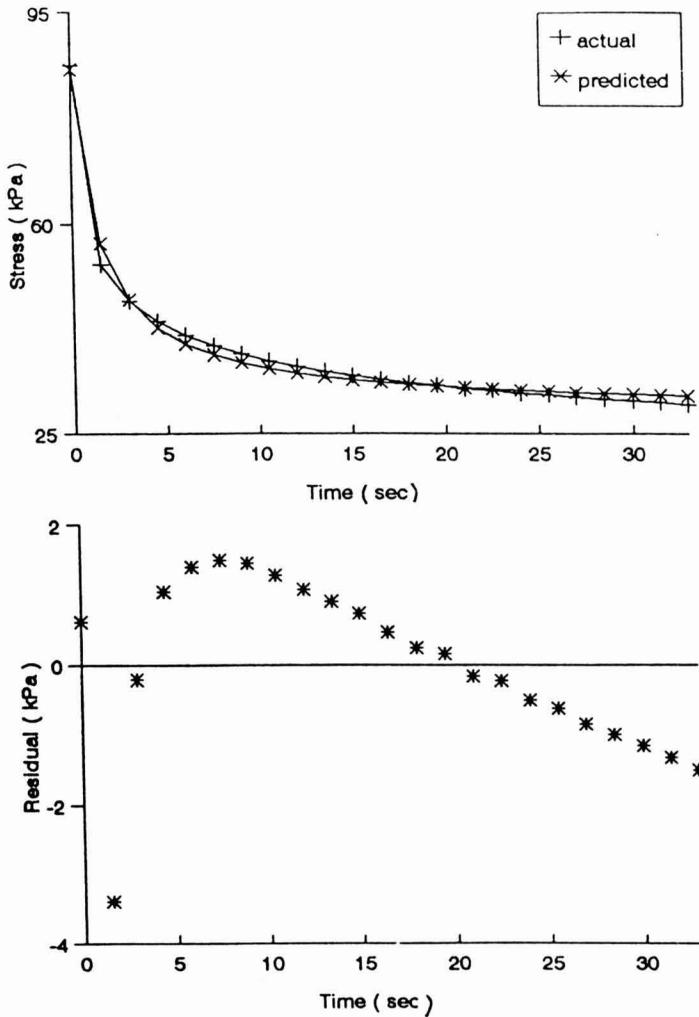


FIG. 5. STRESS RELAXATION CURVE USING THE INVERSE FUNCTION MODEL AND ITS RESIDUAL PLOT

texture. This may be caused by protein denaturation/thermosetting, which can be plasticized by water and lipids (Levine and Slade 1990), or it is likely that starch gelatinization cannot proceed smoothly in microwave baking (Dreese *et al.* 1988; Levine and Slade 1990). It is important to note that the values of G are different from the values of G used as a texture indicator (Table 1). This is due to differences in method of calculation. However, the trend observed was the same: larger value for the microwaved samples.

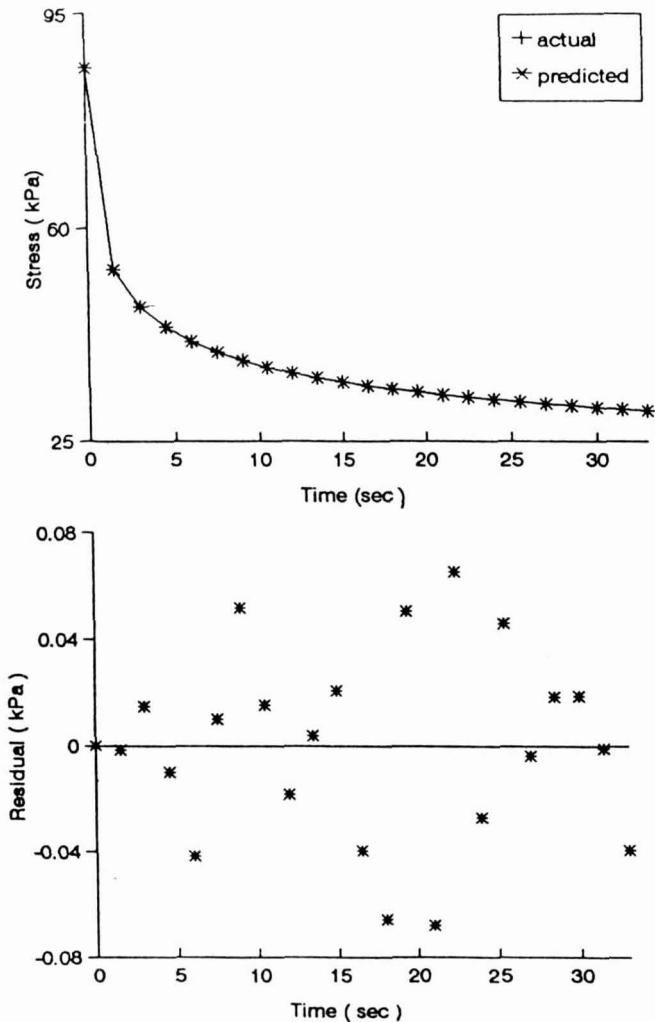


FIG. 6. STRESS RELAXATION CURVE USING THE 5-PARAMETER WIECHERT MODEL AND ITS RESIDUAL PLOT

(3) The estimated viscosities (μ_1 and μ_2 , Wiechert model) for the wheat dough samples baked in the microwave oven were also much larger than those baked in the conventional oven, which offers an experimental support for the high "macroscopic viscosity" in microwave-baked dough hypothesized by Levine and Slade (1990).

These results support the general belief that high viscosity and modulus of elasticity together cause the perceived tough/leathery texture of microwave-baked foods (Levine and Slade 1990; Persaud *et al.* 1990).

TABLE 2.
 MEANS OF PARAMETER ESTIMATES¹ OF THE 5-PARAMETER WIECHERT MODEL
 AND THE INVERSE FUNCTION MODEL FOR CANNED BISCUIT DOUGH BAKED
 IN A MICROWAVE OVEN FOR 50 S AND A CONVENTIONAL OVEN FOR 10 MIN

parameter	Wiechert		Inverse Function	
	microwave	conventional	microwave	conventional
k (dimensionless)	--	--	0.92 a	0.69 b
G _e (kPa)	158.63	29.19	154.58	29.21
G (kPa)	392.78	81.86	393.38	80.57
G ₁ (kPa)	243.87	50.83	--	--
G ₂ (kPa)	148.91	31.03	--	--
μ ₁ (kPa*s)	161.51	41.53	--	--
μ ₂ (kPa*s)	1953.19	598.30	--	--
t ₁ ² (seconds)	0.66	0.82	--	--
t ₂ (seconds)	13.12	19.28	--	--

¹ All parameter estimates are significantly ($p < 0.05$) different from 0 ($n \geq 2$).

² Relaxation time $t_i = \mu_i / G_i$.

Although the differences in moisture loss and viscoelastic characteristics of the baked samples have been described, further studies are needed to establish relationships between baking process and thermal and moisture distributions within the samples for different cooking patterns (power setting, power level, holding time) and sample size. This line of work is currently in progress. Preliminary data on thermal histories of the microwaved samples for this study show that the center temperature reached a value of 98C in the first 10 s with

a maximum of 130C at the end of baking. The surface temperature reached a maximum of 110C with the microwave oven working on a continuous mode at full power level (Naikar and Castell-Perez 1995). The effect of the inverse temperature gradient within the microwaved sample on the gelatinization process and gluten denaturation should be evaluated with structural studies.

CONCLUSIONS

Microwave heating of chemically leavened, canned biscuit dough results in a baked product with tough and leathery texture, associated with a high modulus of elasticity and ratio of elasticity to viscosity. Baking the dough samples for 50 s in the microwave at full power with similar textural characteristics results in a product (modulus of elasticity, weight loss and density) than samples baked in a conventional oven for 10 min. Further study is necessary to determine the effect of surface changes on texture attributes and the rheological effects from crust, cooked and uncooked portions of the dough using fundamental approaches.

ACKNOWLEDGMENT

Financial support for this work was obtained from the USAID Peanut Collaborative Research Support Program (USAID Grant No. DAN-4048-G-00-0041-00).

REFERENCES

- BALE, R. and MULLER, H.G. 1970. Application of the statistical theory of rubber elasticity to the effect of heat on wheat gluten. *J. Food Technol.* 5, 295-300.
- BILIADERIS, C.G. and TONOGAI, J.R. 1991. Influence of lipids on the thermal and mechanical properties of concentrated starch gels. *J. Agric. Food Chem.* 39, 833-840.
- BLOKSMA, A.H. 1990a. Rheology of the bread making process. *Cereal Foods World* 35(2), 228-236.
- BLOKSMA, A.H. 1990b. Dough structure, dough rheology and baking quality. *Cereal Foods World* 35(2), 237-244.
- CASTELL-PEREZ, M.E. and STEFFE, J.F. 1992. Viscoelastic Properties of Dough. Ch.3. In *Viscoelastic Properties of Foods*. (M.A. Rao and J.F. Steffe, eds.) pp. 77-102. Elsevier Applied Science, London.

- DIEFES, H.A., RIZVI, S.S.H. and BARTSCH, J.A. 1993. Rheological behavior of frozen and thawed low-moisture, part-skim Mozzarella cheese. *J. Food Sci.* 58, 764–768.
- DREESE, P.C., FAUBIN, J.M. and HOSENEY, R.C. 1988. Dynamic rheological properties of flour, gluten and gluten-starch dough. (1) Temperature dependent changes during heating. *Cereal Chem.* 65, 348–353.
- ELIASSON, A.C. 1990. Rheological Properties of Cereal Proteins. Ch. 3. In *Dough Rheology and Baked Product Texture*. (H. Faridi and J.M. Faubin, eds.) pp. 157–308. Chapman & Hall, New York.
- FINNEY, K.F., MORRIS, V.H. and YAMAZAKI, W.T. 1949. Effect of varying quantities of sugar, shortening and ammonium bicarbonate on spreading and top grain of sugar-snap cookies. *Cereal Chem.* 26, 38–41.
- GIESE, J. 1992. Advances in microwave food processing. *Food Technol.* 46(9), 118–123.
- INSTRON CORP. 1986. *Instron Universal Testing Instrument (Model 1011) Operating Instruction*. Manual No. M10-1011-1(B). Instron Corp. Canton, MA.
- LEVINE, H. and SLADE, L. 1990. Influences of glassy and rubbery states on the thermal, mechanical and structural properties of dough and baked products. Ch. 5. In *Dough Rheology and Baked Product Texture*. (H. Faridi and J.M. Faubin, eds.) pp. 157–308, Chapman & Hall, New York.
- MATZ, S.A. 1960. *Bakery Technology and Engineering*. Chapman & Hall, New York.
- NAIKAR, S. and CASTELL-PEREZ, M.E. 1995. Understanding the Rheological Changes of Microwaved Biscuit Dough. CoFE 91–96.
- NOLAN, E.J. 1987. Stress relaxation of stored stirred Cheddar curd. *J. Texture Studies* 18, 273–280.
- PAN, B. and CASTELL-PEREZ, M.E. 1994. Residual analysis of stress relaxation models for wheat dough. Paper No. 24E-1, presented July 24–29, at the IFT annual meeting at Atlanta.
- PELEG, M. 1980. Linearization of relaxation and creep curves of solid biological materials. *J. Rheology* 24, 458–463.
- PELEG, M. and POLLAK, N. 1982. The problem of equilibrium conditions in stress relaxation analyses of solid foods. *J. Texture Studies* 13, 1–11.
- PERSAUD, J.N., FAUBION, J.M. and PONTE, J.G. Jr. 1990. Dynamic rheological properties of bread crumb. II. Effects of surfactants and reheating. *Cereal Chem.* 67(2), 182–187.
- SAS INSTITUTE, INC. 1985. *SAS User's Guide: Statistics, Ver. 5 Ed.*, SAS Institute, Cary, NC.
- SHUKLA, T.P. 1993. Bread and bread-like dough formulations for the microwave. *Cereal Foods World* 38(2), 95–96.
- SPSS, INC. 1988. *SPSS-X™ User's Guide, 3rd Ed.* SPSS, Chicago, IL.

- TSCHOEGL, N.W. 1989. *The Phenomenological Theory of Linear Viscoelastic Behavior: An Introduction* pp. 1092–1121, Springer-Verlag, Berlin.
- UMBACH, S.L., DAVIS, E.A., GORDON, J. and CALLAGHAN, P.T. 1992. Water self-diffusion coefficients and dielectric properties determined for starch-gluten-water mixtures by microwave and by conventional methods. *Cereal Chem.* 69(6), 637–642.

ANALYSIS OF MASS TRANSFER IN OSMOTIC DEHYDRATION BASED ON PROFILES OF CONCENTRATION, SHRINKAGE, TRANSMEMBRANE FLUX AND BULK FLOW VELOCITY IN THE DOMAIN OF TIME AND SPACE

ZHIMING YAO¹

*Alberta Food Processing
Development Centre
6309-45 Street
Leduc, AB T9E 7C5 Canada*

AND

MARC LE MAGUER

*Department of Food Science
University of Guelph
Guelph, ON N1G 2W1 Canada*

Accepted for Publication February 10, 1997

ABSTRACT

An analysis of mass transfer mechanisms in osmotic dehydration was carried out by examining the profiles of concentration, shrinkage, transmembrane flux and bulk flow velocity in the domain of time and space. The profiles were obtained through simulations using a computer simulation model that described mass transfer in osmotic dehydration based on cellular structure. It was shown that bulk flow was the main resistance for solute penetration, and the magnitude of bulk flow was affected not only by the transmembrane flux, but by internal cellular structure changes. Since bulk flow often played an important role in mass transfer during osmotic dehydration, precautions should be taken when interpreting mass transfer in osmotic dehydration using a simple pure diffusion theory.

INTRODUCTION

Osmotic dehydration is a water removal process that involves immersing high moisture content materials in an osmotic solution. In this process, there are

¹Corresponding author

at least two simultaneous flows: the solids in the solution penetrate into the material, and water flows out of the material into the solution. Osmotic dehydration has, therefore, been recently referred to as a "water removal and solute impregnation soaking process" (Raoult-Wack *et al.* 1994). It is a useful technique in the food industry for partial concentration of cellular material, like fruits and vegetables, because it offers minimized heat damage (Ponting *et al.* 1966; Contreras and Smyrl 1981), increased retention of volatile and pigments (Flink and Karel 1970), and improved textural quality of dehydrated products (Shipman *et al.* 1972).

The mechanism of mass transfer in osmotic dehydration is complicated and still at the investigative stage (Yao 1994). When a cellular material is immersed in an osmotic solution, the solute penetrates into the tissue along the extracellular volume first. The selective properties of the cell membrane restrict the solute partially or fully from entering the intracellular volume (depending on the solute characteristics), but allow water to pass through easily. The increasing solute concentration in the extracellular volume destroys the equilibrium across the cell membrane and induces a transmembrane flux of water in the direction from the intracellular volume to the extracellular volume. The transmembrane flux tries to bring the cell to a new equilibrium state by concentrating the solution in the intracellular volume and diluting the solution in the extracellular volume. Since the water coming out from the intracellular volume has to flow out along the extracellular volume, the water forms an outflowing bulk flow starting from the center and accumulating along the way towards the surface. The bulk flow opposes the solute penetration and sharpens the concentration gradient. Yao and Le Maguer (1996a) demonstrated that the bulk flow could transport up to 90% of the water removed during osmotic dehydration of potatoes with mannitol solution, and wash back about 60% of the mannitol diffused in. In addition, the shrinkage of the whole tissue and the internal rearrangement of the cellular structure makes the analysis of the osmotic dehydration process more complex.

The driving force for water removal in osmotic dehydration is the chemical potential difference of water across the cell membrane, and this difference is caused by the changing solute concentration in the extracellular volume. The solute concentration in the extracellular volume is a net result of solute diffusion from the osmotic solution into the tissue, dilution by transmembrane water flux, and washout by bulk flow. The concentration, therefore, varies with time and position. In addition, the concentration determined through experiments is the lumped concentration of tissue at a specific position, which is different from the concentration in the extracellular volume. Even the lumped concentration profiles are quite limited (Yao 1994). Unfortunately, there is no information in the literature concerning how bulk flow and transmembrane flux vary with time and position in the extracellular volume. This lack of information makes accurate modeling of mass transfer in osmotic dehydration difficult, greatly

limiting the application of the osmotic dehydration processes in the food industry.

The objective of this paper was to present a detailed analysis of mass transfer mechanisms in osmotic dehydration by examining the profiles of several dependent variables as a function of time and position. The dependent variables investigated included: the concentration of solute in the extracellular volume, the cell stage status which indicated changes in internal cellular structure, the cross-sectional area of the extracellular volume, transmembrane water flux, and bulk flow velocity (volume average velocity).

MATERIALS AND METHODS

The profiles used in the analysis of mass transfer in osmotic dehydration were obtained using a mathematical simulation model developed by Yao and Le Maguer (1996b, 1997a). The model was mechanistic and based on cellular structure. The finite element method was incorporated in the model as a numerical tool to solve partial differential equations. The model provided a mathematical description of the changes with time and position of concentrations in the intracellular and extracellular volumes, bulk flow in the extracellular volume, transmembrane flux and shrinkage. The model was verified against experimental data and shown to successfully represent mass transfer in cellular tissue immersed in osmotic solutions (Yao and Le Maguer 1997a).

Potato slices, 0.001 m thick, immersed in 0.535 kmol/m³ mannitol solution at 20C was simulated. The potato slices were so thin that the edge effect could be ignored, and one-dimensional mass transfer in the thickness direction could be assumed. The one-dimensional case was easy to manipulate mathematically, and allowed the analysis of the general mass transfer mechanism, rather than focusing on individual cases. Mannitol was assumed to be membrane impermeable due to its large molecular size (Stuart 1973). The physical properties of potatoes and transport parameters used in the simulation were the same as those used by Yao and Le Maguer (1997a, 1997b).

Taking advantage of system symmetry, only half the thickness of the potato slice was considered. The half-potato slice was then divided into 1000 linear elements in the thickness direction with dense mesh near the interface between the solution and slice to deal with the large concentration gradient in this region. The initial simulation time step was 0.001 s and the time step was increased by 10% until the maximum time step of 1 s was reached. The total number of elements and the maximum time step were chosen to ensure the convergence of the numerical solution, i.e., the refinement of the mesh and decrease in the time step do not affect the mathematical solution significantly.

RESULTS

The independent variables (position and time) were plotted in dimensionless form in all figures. The distance in the thickness direction measured from the symmetrical plane divided by the half thickness of the slice at that moment was used as dimensionless distance. Therefore the dimensionless distance included the shrinkage of the tissue. The dimensionless time was the ratio of time to an equivalent diffusion time corresponding to the initial conditions, i.e., the square of initial half thickness of the slice divided by the diffusivity of mannitol at infinite dilution. The dimensionless time was similar to the Fourier number for mass transfer.

Concentration in the Extracellular Volume

The dimensionless mannitol concentration in the extracellular volume was plotted in Fig. 1 versus dimensionless distance and time. The dimensionless concentration was the ratio of the concentration at time t to the concentration at time infinity or the concentration in the solution.

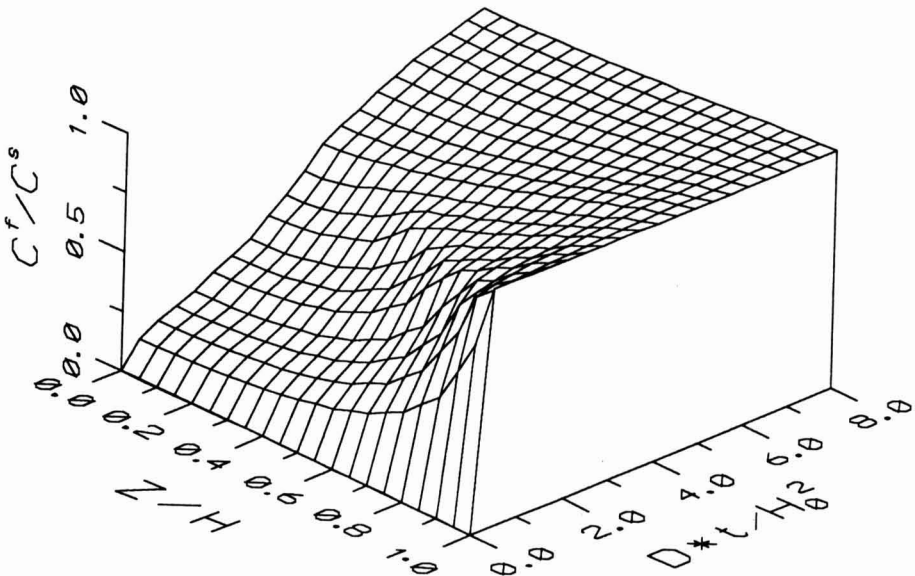


FIG. 1. CONCENTRATION PROFILE OF MANNITOL IN 0.001 m THICK POTATO TISSUE SLICES IMMERSED IN 0.535 kmol/m³ MANNITOL SOLUTION (C^f - Concentration of mannitol in the extracellular volume; C^s - Concentration of mannitol in the osmotic solution; Z - Distance in the thickness direction measured from the symmetrical plane; H - Half thickness of the tissue slice; D - Diffusivity of mannitol at infinite dilution; t - Time; H_0 - Initial half thickness of the tissue slice).

At a specific time, in general, there were three distinct regions on the graph (Fig. 1). There was a flat high concentration region on the right, a flat low concentration region on the left, and in between, a transient region with a steep concentration gradient. The location of the transient region moved from the surface ($Z/H = 1$ in Fig. 1) towards the symmetrical plane ($Z/H = 0$) as the dehydration progressed. As it moved towards the symmetrical plane, the transient region became wider, and the concentration gradient decreased. The high concentration region was absent at the beginning, and the low concentration and transient regions disappeared at the end of the process.

Cell Stage Status

Tissue cells in osmotic dehydration undergo three stages (Marcotte and Le Maguer 1991). Stage I starts from full turgor to incipient plasmolysis or isotonicity. At this stage, cell wall is under pressure and any water loss results in a decrease of intracellular volume but the extracellular volume is constant at a minimum. Stage II proceeds from the incipient plasmolysis to the critical state point where the cell membrane starts to pull away from the cell wall. At this stage, the cell wall is under tension and any water loss from the intracellular volume is gained by the extracellular volume. The extracellular volume in stage II increases from its minimum to a maximum but the total volume is constant. Stage III follows stage II and the extracellular volume remains constant at its maximum. The decrease of the intracellular volume is equal to the decrease of the total volume.

The stage status of cells was an important parameter that characterized the changes in cross-sectional area and therefore, was plotted in Fig. 2 as a function of dimensionless time and position. Initially, all cells were in stage I. However after contacting with osmotic solution, the cells near the surface reached stage II first, quickly passing this stage II, entering stage III. The last cells entering stage II were the cells near the symmetrical plane ($Z/H = 0$) and those cells stayed in stage II the longest. Similar to what was observed with the transient region of the concentration profile in Fig. 1, the location of stage II moved from the surface towards the symmetrical plane. The time that cells stayed in stage II increased as the process continued. The low concentration region in Fig. 1 corresponded to the region where cells were in stage I, the transient region to stage II, and the high concentration zone to stage III.

Cross-Sectional Area of Free Volume

The extracellular volume could be divided into cell wall fiber volume and free volume (empty space in the extracellular volume). The variation of the free volume was exactly the same as the extracellular volume because the cell wall fiber volume was constant. The free volume was the true flowing channel and

had a strong impact on the bulk flow velocity, an important parameter in the analysis of mass transfer in osmotic dehydration (Yao and Le Maguer 1996a).

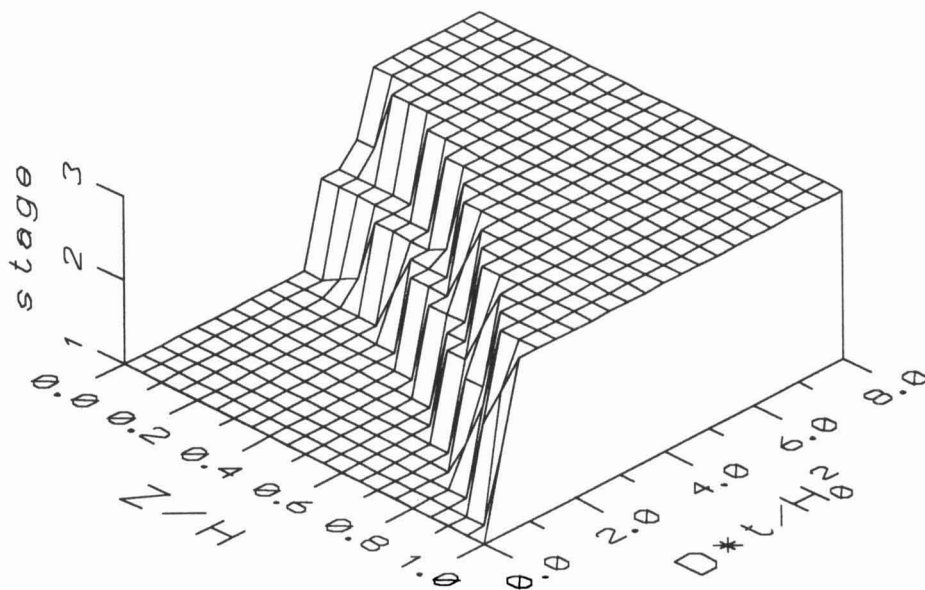


FIG. 2. STAGE STATUS OF CELLS IN 0.001 m THICK POTATO TISSUE SLICES
IMMERSED IN 0.535 kmol/m³ MANNITOL SOLUTION
(Z - Distance in the thickness direction measured from the symmetrical plane; H - Half thickness
of the tissue slice; D - Diffusivity of mannitol at infinite dilution; t - Time;
H₀ - Initial half thickness of the tissue slice).

The variation of the cross-sectional area of the free volume against time and position was simulated and shown in Fig. 3. The cross-sectional area of the free volume was plotted as the ratio of the cross-sectional area of the free volume at time t to its initial value. Similar to Fig. 1, there were three regions in Fig. 3. A low value region (ratio = 1) on the left corresponded to the low concentration region in Fig. 1 where cells were in stage I was evident, followed by a transition region corresponded to the steep gradient zone in Fig. 1 where cells were in stage II. The free volume increased quickly from a small to a large value as cells passing stage II. A high value region (about 3.6 in Fig. 3) corresponded to the high concentration region in Fig. 1 where cells were in stage III. The increase in the cross-sectional area was most rapid at the surface and slowest at the symmetrical plane.

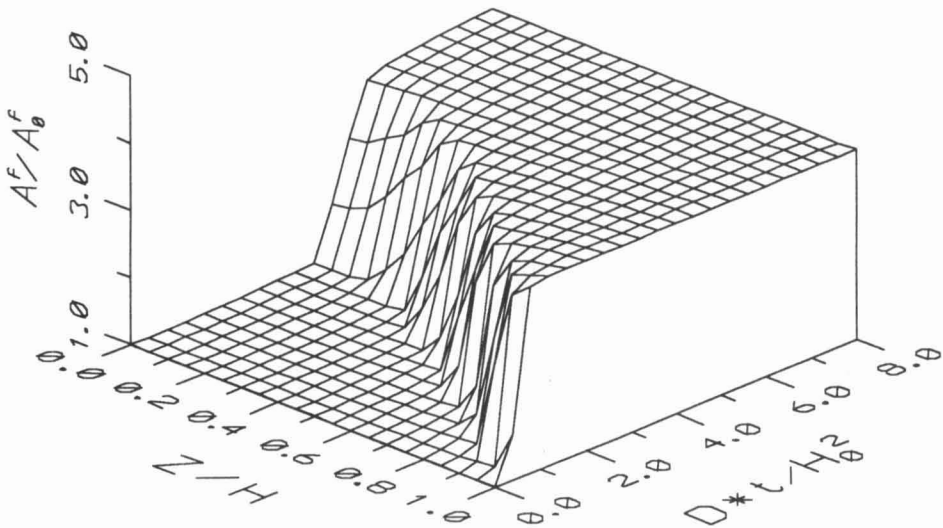


FIG. 3. CROSS-SECTIONAL AREA OF THE FREE VOLUME IN 0.001 m THICK POTATO TISSUE SLICES IMMERSSED IN 0.535 kmol/m³ MANNITOL SOLUTION
 (A^f - Cross-sectional area of the free volume; A_0^f - Initial Cross-sectional area of the free volume; Z - Distance in the thickness direction measured from the symmetrical plane; H - Half thickness of the tissue slice; D - Diffusivity of mannitol at infinite dilution; t - Time; H_0 - Initial half thickness of the tissue slice).

Transmembrane Water Flux

Transmembrane water flux of water is important in the analysis of mass transfer in osmotic dehydration because it indicates the amount of water removed from the intracellular volume where up to 90% of tissue water is located (Nobel 1983). The transmembrane flux forms a bulk flow in the direction from the tissue to the osmotic solution, and the presence of this bulk flow greatly complicates the modelling of osmotic dehydration processes (Yao and Le Maguer 1996a,b). Analysis of transmembrane flux is fundamental to the study of bulk flow in osmotic dehydration.

The transmembrane flux as a function of dimensionless time and distance was shown in Fig. 4. At a particular location, the transmembrane flux increased from zero at the beginning to a maximum and then decreased to zero. The peak, and the rates of the increase and decrease of the transmembrane flux were the highest at the surface ($Z/H = 1$) and lowest at the symmetrical plane ($Z/H =$

0). All cells lost the same amount of water through the membrane to reach equilibrium, regardless of their locations. That meant that the area under the curve along the time axis was the same at all locations in the tissue. However, different cells took different amounts of time to reach this point, depending on their location. The closer the cells were to the interface, the larger and shorter-lasting the transmembrane flux, and vice versa. The location of the maximum of the transmembrane flux (the ridge) corresponded to the beginning of the transient region in Fig. 1 where cells were at the interface between stage I and II.

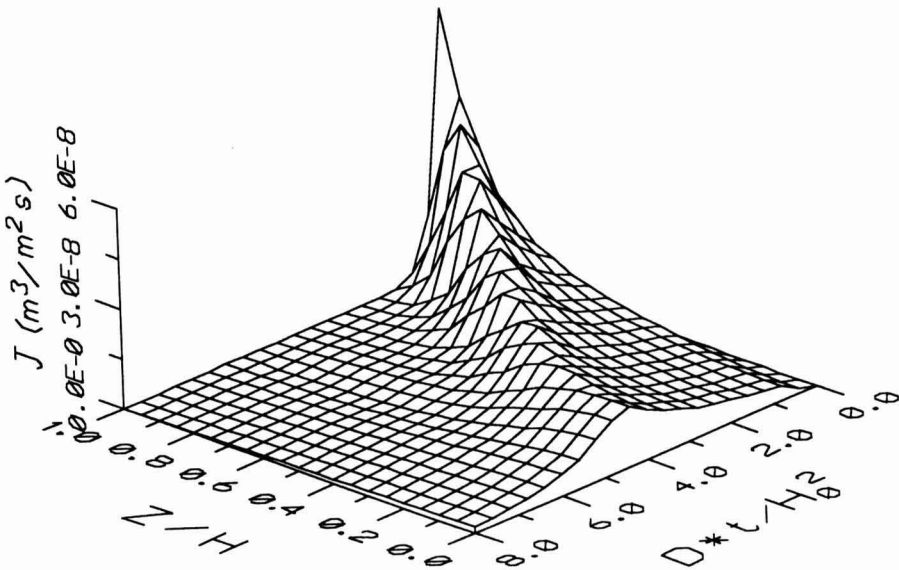


FIG. 4. FLUX OF WATER ACROSS THE CELL MEMBRANE IN 0.001 m POTATO TISSUE SLICES IMMERSSED IN 0.535 kmol/m³ MANNITOL SOLUTION (J - Water flux of water across the cell membrane; Z - Distance in the thickness direction measured from the symmetrical plane; H - Half thickness of the tissue slice; D - Diffusivity of mannitol at infinite dilution; t - Time; H₀ - Initial half thickness of the tissue slice).

Bulk Flow Velocity

As mentioned before, bulk flow played an important role in osmotic dehydration. The bulk flow velocity (volume average velocity) determined the amount of solutes washed out, and was affected by the transmembrane flux in the whole tissue and the change of the cross-sectional area of the free volume in the extracellular volume.

The bulk flow velocity versus dimensionless time and distance was simulated and then plotted in Fig. 5. At the beginning, the bulk flow velocity increased from zero at the symmetrical plane ($Z/H = 0$) to a maximum near the surface ($Z/H = 1$). Later, the velocity reached a peak somewhere between the symmetrical plane and the surface. After this peak, it reduced to a very small value, increasing only slightly afterwards. The location of the peak was shifted from the surface towards the symmetrical plane as the process continued, and disappeared at a dimensionless time of about five. Meanwhile, the peak value decreased with increasing time. After a dimensionless time of approximately five, the velocity increased very slowly from zero at the symmetrical plane until it reached the surface.

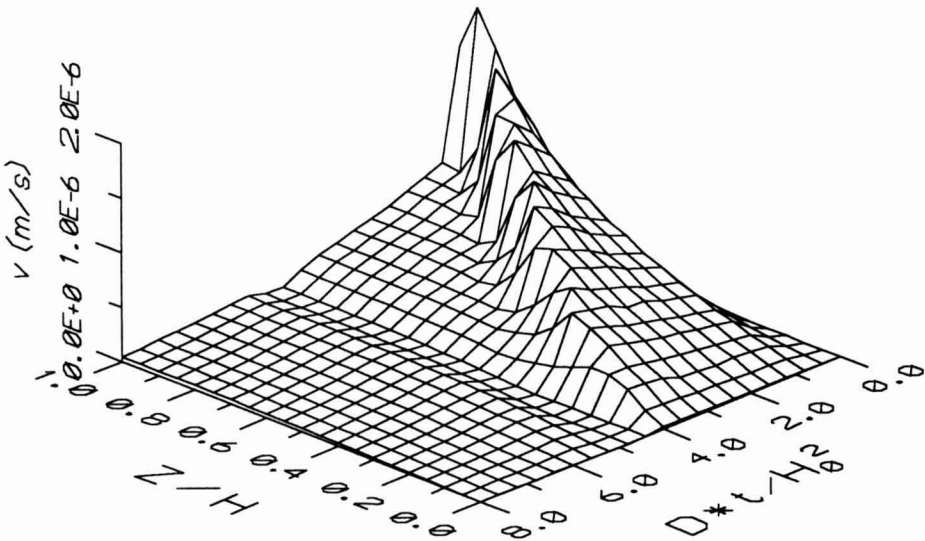


FIG. 5. BULK FLOW VELOCITY IN THE EXTRACELLULAR VOLUME OF 0.001 m THICK POTATO TISSUE SLICES IMMERSSED IN 0.535 kmol/m³ MANNITOL SOLUTION (v - Bulk flow velocity; Z - Distance in the thickness direction measured from the symmetrical plane; H - Half thickness of the tissue slice; D - Diffusivity of mannitol at infinite dilution; t - Time; H_0 - Initial half thickness of the tissue slice).

There were three regions in Fig. 5, one flat and low velocity region on the left, which corresponds to the flat high concentration region on the right of Fig. 1 where cells were in stage III. On the right of Fig. 5, there was a region where the velocity increased continuously, a region matching the low concentration region in Fig. 1 (left) where the cells were in stage I. A peak, located between

these two regions, matched the transient region in the concentration plot (Fig. 1).

DISCUSSION

Effect of Bulk Flow on Concentration Gradient

Because we are dealing exclusively with the concentration within the free volume, bulk flow is the main reason for the difference between the concentration profile in osmotic dehydration and pure diffusion. The concentration gradient $\partial C_i/\partial z$ of species i along the thickness direction is related to the bulk flow velocity (v) through the following equation:

$$N_i = C_i v - D_i \frac{\partial C_i}{\partial z} \quad (1)$$

where N_i is the flux of species i referred to the stationary frame and D_i the diffusion coefficient of species i . For mannitol penetrating from solution to tissue, the bulk flow and the diffusion flux occur in opposite directions (bulk flow from tissue to solution and diffusion from solution to the tissue). Both terms in Eq. (1) are positive but the diffusion term (second term in Eq. 1) is larger than the bulk flow term (first term). Therefore, the net flux, N_i , is negative, i.e., flowing from the solution to the tissue because the direction from the tissue to solution is defined as positive. Consequently, for a constant flux (N_i), the larger the bulk flow velocity (increase in the first term), the higher the gradient (increase in the second term), and vice versa. This is consistent with the finding by Yao and Le Maguer (1996a) that the diffusion component is proportionally associated with bulk flow component transported. Even though diffusion is the cause of bulk flow, bulk flow controls diffusion by affecting the concentration gradient.

In the beginning of the transient region where cells are just entering stage II, the bulk flow velocity is largest at a specific position (Fig. 5), which results in the steepest gradient in this region as shown in Fig. 1. As the transient region moves from the surface towards the center, the peak of the bulk flow velocity decreases (Fig. 5), resulting in a reduced steepness of the concentration curve in the transient zone as shown in Fig. 1. By comparison, a pure diffusion case would have a dimensionless concentration at the center line of 0.6 for dimensionless time of 0.5 versus the value of 0.1 currently obtained. By the time the dimensionless time would have reached 1.5, the total slab would be practically in equilibrium with the solution for pure diffusion. By contrast, it would take a value of 5.5 to achieve the same result (or 3.7 times larger) with the presence of bulk flow. The influence of the bulk flow is consequently

considerable and indicates that attempting to interpret osmotically driven processes on the basis of pure diffusion would lead to serious underestimation of the time.

It is, however, worth noting that this is similar to the behavior observed in a packed bed where a step function in concentration is applied at the entrance of the bed. It is diffusion which is responsible for spreading the boundary of the travelling high concentration ridge. Here, the bulk flow generated by the cells through water loss plays the role of the convection velocity obtained from the pump in a packed bed system. A ridge of high concentration travels down from the surface to the center and spreads as time passes, a direct result of diffusion. It could be anticipated, therefore, that for a plug flow pattern, fast diffusing molecules would lead to a wider front. However, because of the interaction between the bulk flow velocity and the cell membrane flux, the phenomenon is not as straight forward as in a packed bed.

Figure 1 shows that the flat high concentration region is narrow at the beginning and located close to the surface, which agrees with the conclusion that solute gain is first limited to a thin layer near the interface (Bolin *et al.* 1983; Lenart and Flink 1984). Except for the transient region where the steep concentration gradient occurs, the concentration does not vary much. This is the reason why osmotic dehydration can be simplified as a bi-compartment model (Raoult-Wack *et al.* 1991). The transient region corresponds to the interface between the two compartments. The areas beside the transient region correspond to the two compartments where the concentration was assumed as constant. They consider the volume of the two compartments to be fixed, while the concentration curve shows that the volume of the flat high concentration region increases and the volume of the low concentration region decreases with time.

Bulk Flow Analysis

The bulk flow is related to the transmembrane flux and changes in the cross-sectional area of the free volume as (Yao and Le Maguer 1996b):

$$(vA)|_z = \int_0^z (J_1 \bar{v}_1) E \, dz - \int_0^z \frac{\partial A}{\partial t} dz \quad (2)$$

where v is the bulk flow velocity, A the cross sectional area of the free volume, J_1 the transmembrane water flux, \bar{v}_1 the partial molal volume of water, E the area of the cell membrane per unit thickness and t time. Since the only permeable species is water in this simulation we have only component 1 to deal with. The left-hand side of the equation represents the volume flow rate at position z . The first term on the right hand side is the total volume of water

extracted from the intracellular volume in the region between the symmetrical plane ($z = 0$) and position z . The second term is the contribution by the change of the free volume with respect to time in the same region.

For a particular tissue, the transmembrane volume flux is determined by the chemical potential difference across the cell membrane. As the solute in the solution penetrates into the tissue, the chemical potential of water in the extracellular volume decreases, which leads to the outflow of water from the intracellular to extracellular volume. The outflow of water concentrates the solution in the intracellular volume and caused the chemical potential of water in the intracellular volume to decrease. On the other hand, the outflow of water reduces the concentration and increases the chemical potential of water in the extracellular volume. The penetration of solute is, therefore, counterbalanced by the transmembrane water flux which tries to restore a new equilibrium. Obviously the membrane permeability would be an important factor in controlling this process.

Figure 1 shows that the highest rate of mannitol concentration rise with time occurs at the surface and the lowest at the symmetrical plane. This leads to the pattern of transmembrane flux shown in Fig. 4. The peak maximum is located at the surface and the peak minimum is at the symmetrical plane. The peak of the transmembrane flux is caused by the rapid increase of the mannitol concentration in the free volume. The steep gradient of mannitol concentration is located where the cells enter stage II (Fig. 1 and 2). Therefore, the transmembrane flux peaks, the steep gradient of mannitol concentration correspond to where the cells enter stage II.

The second term on the right hand side of Eq. (2) will disappear when cells are in stage I and III because the cross-sectional area of the extracellular volume in these stages is constant. The cumulative transmembrane fluxes between the symmetrical plane and position z will contribute to the bulk flow at position z . In stage I, the cross-sectional area of the free volume is constant at its minimum. Then the bulk flow velocity increases from zero at the symmetrical plane to its maximum before entering stage II. In stage II, the cross-sectional area of the free volume increases rapidly to its maximum (it increased 3.6 times in this analysis). This results in the bulk flow velocity falling down quickly from its maximum to a small value as the cells pass through stage II (Fig. 3). Due to the large cross-sectional area of the free volume, the bulk flow velocity in the area where cells are in stage III is very low and increases slightly from the ridge to the surface.

CONCLUSIONS

The presence of bulk flow makes the mass transfer in osmotic dehydration much more complex than what would be observed with pure diffusion. The bulk

flow not only retards the penetration of solute, but the water loss since the presence of solute in the extracellular volume is the driving force for water removal. The rate controlling region for solute penetration is where the cells just pass incipient plasmolysis and the bulk flow velocity is the largest. The bulk flow, therefore, has to be considered in the modelling of osmotic dehydration. More research is required to accurately predict the bulk flow quantitatively because it is affected not only by the transmembrane flux, but by internal cellular structure changes.

NOMENCLATURE

- A cross-sectional area of the free volume (m^2)
 C_i concentration of species i ($kmol/m^3$)
 D_i diffusivity of species i (m^2/s)
 E area of cell membrane per unit thickness (m)
 J_1 transmembrane water flux ($kmol/m^2 \cdot s$)
 N_i flux of species i referred to a fixed frame ($kmol/m^2 \cdot s$)
 t time (s)
 v bulk flow velocity (m/s)
 \bar{v}_1 partial molal volume of water ($m^3/kmol$)
 z coordinate of in the direction of tissue thickness (m)

ACKNOWLEDGMENTS

This project was supported by a grant from the Natural Science and Engineering Research Council of Canada. The authors thank Dr. Robert W. Lencki for his assistance in preparing this manuscript.

REFERENCES

- BOLIN, H.R., HUXSOLL, C.C., JACKSON, R. and NG, K.C. 1983. Effect of osmotic agents and concentration on fruit quality. *J. Food Sci.* **48**, 202-205.
- CONTRERAS, J.E. and SMYRL, T.G. 1981. An evaluation of osmotic concentration of apple rings using corn syrup solids solutions. *Can. Inst. Food Sci. Technol. J.* **14**(4), 310-314.
- FLINK, J.M. and KAREL, M. 1970. Effects of process variables in retention of volatiles in freeze-drying. *J. Food Sci.* **35**, 444-447.

- LENART, A. and FLINK, J.M. 1984. Osmotic concentration of potato. II. Spatial distribution of the osmotic effect. *J. Food Technol.* 19, 65–89.
- MARCOTTE, M. and LE MAGUER, M. 1991. Repartition of water in plant tissues subjected to osmotic processes. *J. Food Process Engineering*, 13, 297–320.
- NOBEL, P.S. 1983. *Biophysical Plant Physiology and Ecology*. W.H. Freeman and Company.
- PONTING, J.D., WATTERS, G.G., FORREY, R.R., JACKSON, R. and STANLEY, W.L. 1966. Osmotic dehydration of fruits. *J. Food Technol.* 20, 125–128.
- RAOULT-WACK, A., PETITDEMANGE, F., GIROUX, F., GUILBERT, S., RIOS, G. and LEBERT, A. 1991. Simultaneous water and solute transport in shrinking media. Part 2. A compartmental model for dewatering and impregnation soaking processes. *Drying Technol.* 9(3), 613–630.
- RAOULT-WACK, A., RIOS, G., SAUREL, R., GIROUX, F. and GUILBERT, S. 1994. Modelling of dewatering and impregnation soaking process (osmotic dehydration). *Food Res. Int.* 27, 207–209.
- SHIPMAN, J.W., RAHMAN, A.R., SEGARS, R.A., KASPSALIS, J.G. and WEST, D.E. 1972. Improvement of the texture of dehydrated celery by glycerol treatment. *J. Food Sci.* 37, 568–571.
- STUART, D.M. 1973. Reduction of water permeability in potato tuber slices by cyanide, ammonia, 2,4-dinitrophenol, and oligomycin and its reversal by adenosine 5'-triphosphate and cytidine 5'-triphosphate. *Plant Physiol.* 51, 485–488.
- YAO, Z. 1994. Modelling and simulation of mass transfer in osmotic dehydration processes. Ph.D. Thesis, Food Science Department, University of Guelph, Canada.
- YAO, Z. and LE MAGUER, M. 1996a. Osmotic dehydration: An analysis of fluxes and shrinkage in cellular structure. *Transactions of the ASAE* 39 (6), 2211–2216.
- YAO, Z. and LE MAGUER, M. 1996b. Mathematical modelling and simulation in osmotic dehydration processes. Part I: Conceptual and mathematical model. *J. Food Eng.* 29, 349–360.
- YAO, Z. and LE MAGUER, M. 1997a. Mathematical modelling and simulation in osmotic dehydration processes. Part II: Simulation and verification. *J. Food Eng.* 32, 21–32.
- YAO, Z. and LE MAGUER, M. 1997b. Mathematical modelling and simulation in osmotic dehydration processes. Part III: Parametrical study. *J. Food Eng.* (accepted).

THE THERMAL PROPERTIES OF POTATOES AND CARROTS AS AFFECTED BY THERMAL PROCESSING¹

EDGAR G. MURAKAMI²

*Food and Drug Administration
National Center for Food Safety and Technology
6502 S. Archer Ave.
Summit-Argo, IL 60501*

Accepted for Publication February 12, 1997

ABSTRACT

The effects of processing on the thermal properties of white potatoes and carrots were studied. The test samples were blanched, boiled, cooked and canned. Whole potato tubers were baked to study the effects of starch gelatinization. The thermal conductivity (k) and density (ρ) were measured and the specific heat (c_p) and thermal diffusivity (α) were calculated. Results showed that in general, α initially decreased and then increased during processing. Test samples were found to have a gain in α when their moisture content increased by more than 9%. The α of potatoes decreased after canning and increased after boiling. In carrots, a similar trend was also observed but to a lesser degree. The k of potatoes was unaffected after blanching or cooking. In all the processing treatments of carrots, the k and the c_p increased and the ρ was unaffected. The baking study showed that gelatinization significantly decreased the k of potatoes.

INTRODUCTION

When establishing a thermal process, conservative procedures are used to ensure food safety. In thermal processing of low-acid canned foods, this is satisfied by calculating lethality based on the 'cold spot' temperature. The 'cold spot' is the location in food materials which has the slowest heating rate during the heat treatment. For conduction-heated food products, the 'cold spot' is usually at the center of a particle located near the center of the can and its temperature is measured with a thermocouple. In aseptic processing, where food materials continuously move in a system of pipes, the particulate temperature cannot be measured. An alternative is to predict temperature by using mathemat-

¹ The contents of this paper are solely the opinions of the author and do not necessarily represent the official views of the U.S. Food and Drug Administration.

² Please address correspondence to the author. Phone: (708) 728-4163, Fax: (708) 728-4177

ical models, which require knowledge of the thermal properties. For mathematical models to be conservative, the thermal properties must be measured at an appropriate stage of processing, e.g., raw, blanched, or fully processed, such that the model calculates the process parameters corresponding to the slowest heat transfer. For conduction in particulates, this is the state when the thermal diffusivity (α) of the product is lowest. It should be noted that heat transfer in aseptic systems includes conduction and convection and the heating rate in particulates is dependent on their thermal properties and the velocity profiles around them, which are also affected by their density (ρ). This study considers only the internal heat transfer in food particulates.

In aseptic processing, particulate foods are immersed either in water or in water-based solutions like soup or saline solution. The thermal properties of foods can change by absorbing/desorbing water and solutes and thermally degrading some food components. Raw carrots and potatoes are predominantly made up of water and their dry matter consists mostly of carbohydrates. Because water has higher thermal conductivity (k) than carbohydrates (0.602 vs 0.25 W/m $^{\circ}$ K) (Choi 1985), an increase in water content increases the k of potatoes and carrots. Changes in the concentration of salt in food materials also affects thermal properties. M.W. Kellogg Co. (1955) reported that an increase in salt concentration lowered the k and increased the ρ of saline solution. Murakami (1994) reported that shrimp and scallops blanched in saline solution had lower thermal conductivities than those blanched in water.

Thermal processing can also alter the thermal properties of carrots and potatoes by the thermal degradation of some of their components, such as starch and protein. Lumbago and Hallstrom (1986) reported that potato starch started to gelatinize at 55C and ceased at 75C, with the maximum gelatinization occurring at 66C. Choi (1985) estimated that starch gelatinization decreased the k of carbohydrate solutions by 13%.

Several studies have shown the relative effects of changes and measurement errors in thermal properties on various process parameters. In a simulation of several critical parameters in aseptic processing of particles, Larkin (1990) showed that lethality (F_0) was sensitive to errors in the thermal properties. He calculated that lethality will be underestimated by 10% if ρ is overestimated by 2.5%, if specific heat (c_p) is overestimated by 1.6%, or if k is underestimated by 2.6%. Process time is directly proportional to holding tube length in continuous aseptic processing systems. Simulations by Chandarana *et al.* (1989), Chandarana and Gavin (1989), and Sastry (1986) suggested that a 50% increase in α of particulate food requires a corresponding 29% reduction in holding tube length (Larkin 1990). An error analysis by Lee *et al.* (1990) indicated that a 1.0% overestimation in the α would result in a 0.5% reduction in the calculated process time. Depending on the application, this can be significant since the reported level of accuracy in α measurements varies widely, from $\pm 1\%$ (Knibbe

and Raal 1987) to $\pm 11\%$ (Parson and Mulligan 1978). The accuracy of α measurements is usually lower than k measurements (Nieto de Castro *et al.* 1988).

The thermal properties of potatoes and carrots have been previously studied. Rao *et al.* (1975) reported that the thermal conductivities, densities and thermal diffusivities of five varieties of raw potatoes were 0.533-0.571 W/m^{°K}, 1.04-1.05 g/cc and $0.165-0.184 \times 10^{-6}$ m²/s, respectively. The freshly harvested test samples had a moisture content (X_{wb}) range of 81.2-83.6%wb. Thermal conductivity and thermal diffusivity were measured simultaneously by using the line-heat source technique. Studies have shown that the k of potatoes is not affected by temperature up to 70C (Wang and Brennan 1992) but does increase at 130C (Gratzek and Toledo 1993). For fresh carrots ($X_{wb}=90\%$), Sweat (1974) reported that their k was 0.605 W/m^{°K} and their ρ was 1.04 g/cc. The objective of this study was to determine the effect of thermal processing on the thermal properties of potatoes and carrots.

MATERIALS AND METHODS

Preparation of Carrots and Potatoes

The carrots and the potatoes (White Russet) were bought fresh from a local grocery store and stored in a refrigerator. For comparison, commercially-canned potatoes were included in the study. Commercially-canned carrots were not included because their diameters were too small for the k probe apparatus. The potatoes and carrots were peeled and shaped into cylinders ($D=22.2$ mm, $L \geq 50$ mm) with a cork borer to provide uniform thermal treatment during blanching, cooking and canning. For k measurements of raw and baked potatoes, the ellipsoid tubers were cut in half along the minor axis. The peel was left intact and the exposed areas were covered with a sheet of plastic wrap (low density polyethylene) to minimize moisture loss. The k probe was pierced through the plastic wrap and transferred to several locations in the half tuber for replications. The number of measurements for each half tuber was between 3-5, which was equal to the number of cylindrical test samples that could have been made with a 22.2-mm cork borer. For the baking and canning tests, the k data for raw potatoes were measured from at least four half tubers. For cooking and blanching processes, each potato tuber was cut in half and one-half was used as raw sample and the other half was processed. At least two potato tubers were used in those tests, giving a total of at least 6 replicates for both raw and processed potatoes. For raw carrots, the k determination was conducted with test samples that were at least 22.2 mm in diameter. There were at least five replicates for raw and processed carrots.

The processing operations used simulated the thermal processing of particulate foods. The carrots were blanched and canned and the potatoes were blanched, cooked, canned and baked. Although baking is not one of the unit operations in thermal processing, potatoes were baked in a convection oven to determine the effect of gelatinization without a change in X_{wb} on k . The canned carrots were preblanched in steam kettles (Groen Kettle Co., Elk Grove, IL) before they were placed in tin cans (300 × 404) and sealed using a manual Dixie can sealer (Dixie Canner Equipment Co., Athens, GA). The carrots were retorted in steam using a Dixie vertical still retort. The canned potatoes were prepared using the same procedure except that they were not blanched (Table 1).

TABLE 1.
THE CANNING PROCEDURE AND THE PROCESS DATA
FOR CARROTS AND POTATOES

Samples	Blanching	Retorting
1. Potatoes	None	a. Filled with 2% brine b. Retorted to $F_0=3.7$, 23.5 min i. time = 16.5, 35.0 min ii. $j_h = 1.27$ iii. $f_h = 8.90$
2. Carrots	Boiled in water for 2 min	a. Filled with 2% brine b. Retorted to $F_0=3.7$, 27.9 min i. time = 13.6, 35 min ii. $j_h = 0.80$ iii. $f_h = 7.89$

Note:

$T_r = 121.1$ C (250 F), $T_i = 37.8$ C (100 F),
Can size = 300 x 404, Come up time = 2 min.

The carrots were blanched in boiling 2% saline solution for 4 min and the potatoes in boiling water for 10 min and 2.5 h in a covered aluminum pot. The extended blanching or boiling was used to evaluate the properties of potatoes that had equilibrated during processing. The potatoes were cooked in boiling cream of potato soup (CPS) for 60 min in the same cooking pot to simulate aseptic processing. The CPS was prepared by mixing equal amounts of whole

milk and commercially-available condensed CPS. In another treatment, test samples were preblanched for 10 min in boiling water and then cooked in CPS for 50 min.

The carrots and potatoes were canned following the procedure of Lopez (1987) and the process parameters were determined from heat penetration tests (Table 1). The carrots were pretreated by blanching them in boiling water for 2 min. Tin cans with 2% brine were filled with four pieces of carrots and potatoes. There were 10 cans of each carrots and potatoes. Both carrots and potatoes were given a thermal treatment equivalent to an $F_0=3.7$ min. The process parameters were previously determined by running a heat penetration test for 35 min, as described by Murakami (1994). The carrots used in the heat penetration tests had an $F_0=27.9$ min and the potatoes had $F_0=23.5$ min.

Three whole potato tubers were baked at 205C for 0.5, 1.0, 1.5 and 2.0 h in a convection oven. Each tuber was wrapped in two layers of aluminum foil to avoid moisture loss. Prior to the measurement of thermal properties, the baked potatoes were allowed to cool overnight at room temperature before they were unwrapped.

The paired t-test was used to determine the statistical significance of the various treatments relative to the raw test samples and drift of the k probe. The prepared samples for each thermal treatment were divided into reference and test lots. The reference materials were kept raw and the test materials were processed. Except for the test samples that were canned and baked, comparison between raw and processed samples were based on data that were measured on the same day. For the cooked and blanched potatoes, the raw and processed samples were made from the same tuber and at least two tubers were used in each test. The data presented for raw potatoes and carrots were calculated by combining the measurements from the various processes. Although this approach required repetitive measurements of raw test samples and cannot be used for statistical comparison between the thermal treatments, it has several advantages. It eliminated the errors due to sample-to-sample diversity, storage effects, day-to-day variation of operator efficiency and equipment wear and tear. Moreover, the paired t-test approach also allowed the completion of the various tests over a long period of time. All statistical analysis were performed by using a 2-tailed t-test with a 95% confidence interval. The statistical significance of changes in the values of c_p and α were not evaluated. Because their values were calculated from mathematical models, the corresponding standard deviations and significance of changes in properties could not be determined.

Thermal Properties

The thermal properties studied were thermal conductivity (k), density (ρ), specific heat (c_p) and in some cases, the volumetric expansion (ν) after

processing. Thermal diffusivity (α) was calculated from $k/\rho c_p$. Prior to measurement the processed test samples, except those that were canned, were cooled to room temperature ($\sim 25\text{C}$) for about 2 h in the liquid in which they were processed. The canned test samples were retorted in cream of potato soup (arbitrarily chosen), stored at ambient conditions and analyzed 3 days after processing. All processed test samples were assumed to have sufficient time for temperature and X_{wb} equilibration.

Measurement of Thermal Conductivity and Density

The k was determined by using a PC-based k probe apparatus (Murakami 1994). The k measurement was conducted for 10 s and the power input was fixed at 11.4 W/m. Before the tests were started in a given day, the k apparatus was calibrated with 0.6% water-agar gel. At the end of the day, the system was recalibrated to determine drift. Drift was evaluated by comparing the calibration results using the t-Test (2 tailed, $\alpha' = 0.05$) and it was found that the drift of the system was not significant.

To avoid moisture loss during k measurements, the raw and baked test samples were wrapped in plastic sheets, and the processed test samples were submerged in the liquid in which they were processed. The processed test samples were shaped into cylinders; and to avoid errors with edge effects, their size was maintained at $D = 22.2$ mm and $L \geq 50$ mm. (Murakami 1994; Murakami *et al.* 1996). During the k measurements, it was difficult to place the k probe at the exact geometric center of the cylinders, which caused a potential problem with edge effects. Therefore, a test was devised to evaluate the effects of off-center probe locations. Measurements were made with the k probe positioned at the center ($r = 0$), $r/3$, $r/2$ and $2r/3$. To eliminate the effect of sample-to-sample variations, all four probe locations were evaluated in each cylinder and four different test samples were used. Results showed that the readings from all the off-center probe positions were not different from those taken at the center. It was possible that there were edge effects, especially at $2r/3$, but they were negligibly small since the test samples and the surrounding medium had similar thermal conductivities.

Density and volumetric expansion were measured gravimetrically (Mohsenin 1970) by using a 25-mL pycnometer bottle. The details of the procedure were reported by Murakami (1994). The X_{wb} of all test samples was determined using a vacuum oven set at 96.7C and 13.5 Kpa. and the drying time was at least 20 h, when the test sample weight became constant. The test samples were shredded to small pieces and there were five replicates.

Calculations of Specific Heat, Thermal Diffusivity and Error or Uncertainty

Specific heat was evaluated by taking the sum of the heat contents of the

various food components (i.e., water, protein, fat, carbohydrate, fiber and ash). It was calculated from:

$$c_p = \sum_i X_i^w c_{pi} \quad (1)$$

where:

$$\begin{aligned} c_{pi} &= \text{specific heat of each food component} \\ X_i^w &= \text{weight fraction of each food component} \end{aligned}$$

The c_p values of the various food components were determined at $T=25C$ using the equations developed by Choi (1985). The errors of Choi's (1985) equations were between 2-6%. The composition of carrots and potatoes were calculated from the handbook by Adams (1975). The composition of raw test samples were based on raw and unpeeled materials and the processed test samples on those that had been boiled and pared. The composition was adjusted for the appropriate X_{wb} of the test samples.

The α was determined from the following:

$$\alpha = \frac{k}{\rho c_p} \quad (2)$$

The uncertainties of the measured properties were equal to the standard deviation of the replicates. The uncertainty of the c_p equation was estimated from the standard error of the equation for the carbohydrate which was reported by Choi (1985) to be approximately equal to 6%. For calculated values, Kline and McClintock (1953) (Huggins 1975) suggested that the uncertainty can be derived from the partial differential of the working equation with respect to the various variables. For α , the expression for uncertainty (E_α) was derived from Eq. 2 and the resulting equation is:

$$E_a = \left[\left(\frac{1}{\rho c_p} E_k \right)^2 + \left(\frac{k}{\rho^2 c_p} E_\rho \right)^2 + \left(\frac{k}{\rho c_p^2} E_{c_p} \right)^2 \right]^{1/2} \quad (3)$$

The variables E_k , E_ρ , E_{c_p} are the uncertainties of the k , ρ and c_p , respectively.

RESULTS AND DISCUSSION

The k , X_{wb} and ρ of fresh carrots were found to be 0.569 W/m $^\circ$ K, 87.6 % wb (wet basis) and 1.029 g/cc, respectively (Table 2). The X_{wb} value compares favorably to the data (88.2%wb) published by Adams (1975). Results show that all the thermal treatments significantly changed the k and X_{wb} of carrots but did

not affect the ρ (Table 3). Blanching the carrots in saline solution caused them to absorb a significant amount of water (1.7%), which consequently, increased the k by 1.4%. However, the change in X_{wb} was not high enough to influence the ρ . Compared with the thermal properties of water, the k of raw carrots was 5.5% lower and ρ was 2.9% higher. Thus, during thermal processing when the potential for changes in X_{wb} is high, the k is more sensitive than ρ . This was

TABLE 2.
THERMAL PROPERTIES OF RAW POTATOES AND CARROTS

	Raw Potatoes ^a		Raw Carrots ^a	
	$\bar{x} \pm E^b$	N	$\bar{x} \pm E^b$	N
X_{wb} (%, wb)	77.8±2.3	35	87.6±0.1	5
ρ (g/cc)	1.089±0.022	23	1.029±0.003	10
k (W/m-°K)	0.563±0.007	44	0.569±0.010	17
c_p^c (kJ/kg-°C)	3.603±0.216		3.849±0.231	
α^c (m ² /s, x10 ⁻⁶)	0.144±0.009		0.144±0.009	

^a Evaluated from raw data from all processing operations and were not used to calculate change in the values of properties.

^b E= uncertainty, for ρ and k =standard deviation, for c_p = 6% of c_p , for α = calculated from eqn. 3

^c Calculated.

TABLE 3.
THERMAL PROPERTIES AND VOLUMETRIC EXPANSION
OF BLANCHED AND CANNED CARROTS

	Blanched (2% saline solution, 4 min.)				Canned (F ₀ =27.9)				Canned (F ₀ =3.7)			
	$\bar{X} \pm E^a$	N	$\Delta, \%^b$	r-test ^c	$\bar{X} \pm E^a$	N	$\Delta, \%^b$	r-test ^c	$\bar{X} \pm E^a$	N	$\Delta, \%^b$	r-test ^c
X _{wb} (%, wb)	89.1±0.4	10	1.7	s	93.7±0.1	5	7.0	s	93.5±0.4	5	6.7	s
ρ (g/cc)	1.036±0.016	5	0.4	ns	1.029±0.002	5	-0.2	ns	1.031±0.002	10	-0.1	ns
k (W/m ² ·K)	0.577±0.005	19	1.4	s	0.591±0.006	8	3.8	s	0.589±0.003	22	3.5	s
v (%)	2.3±1.7	4										
C _p ^d (kJ/kg·°C)	3.985±0.234		1.2		4.015±0.241		4.2		4.009±0.241		4.3	
α ^d (m ² /s, x10 ⁻⁶)	0.143±0.009		-0.2		0.143±0.009		-0.2		0.143±0.009		-0.7	

^a E= uncertainty, calculations of E for X_{wb}, ρ and k =standard deviation, for c_p = 6% of c_p, and for α= calculated from eqn. 3

^b Change in values of processed with respect to raw products.

^c Based on 2-tailed t-test at α = 0.05 of raw vs processed products.

^d Calculated

evident in the canned carrots. Although their X_{wb} increased by about 7%, the change in ρ was negligible while in k it was significant. The c_p of carrots increased in all processes, especially after canning when the moisture absorption was high. The α of carrots decreased slightly in all processes.

The average thermal properties of raw white potatoes were calculated by using the values from all unprocessed samples (Table 2). After the standard deviation was taken into account, it was found that the average k , ρ , and α values in this study compared favorably to the values reported by Rao *et al.* (1975). Relative to the thermal properties of water, the k of raw potatoes is 7.3% lower and their ρ is 8.9% higher. This means that when potatoes absorb water, their k and ρ values are more likely to change than carrots. However, in thermal processing of starchy materials the change in k can be counteracted by starch gelatinization, which decreases k .

Blanching the potatoes for 10 min increased their X_{wb} by 5.9% and resulted in a 1.7% decrease in ρ , while the k was unaffected (Table 4). The negligible effect of the increase in moisture on the k of blanched potatoes may have been neutralized by starch gelatinization. The c_p of potatoes after blanching increased and their α decreased. Boiling the potatoes for an extended duration increased their moisture by 9.8% and k by 4.2% and the ρ decreased by 2.3%. The large change in the X_{wb} indicated that the potatoes did not reach equilibrium X_{wb} during the shorter blanching process. Due to the large amount of water absorbed, the c_p of the boiled samples increased. However, due to the decrease in ρ and increase in k , the α increased by 1.1%.

The X_{wb} of potatoes canned to an $F_0=3.7$ min increased by 7.7% (Table 5). The change was high enough to significantly change the ρ but not the k . The longer F_0 treatment caused the test samples to absorb enough moisture to change both the ρ and k . The commercially-canned potatoes had higher X_{wb} than those canned to an $F_0=23.5$ min. The X_{wb} of the commercial potatoes was so high that their k was not significantly different from that of the liquid that it was canned with ($k=0.589 \pm 0.004$ W/m²·K). Results also showed that the k of the liquid from the cans was significantly lower than the plain water. Due to large amounts of moisture absorption, the c_p of all canned test samples increased by more than 4%. This resulted in decreases in α for the samples canned in the study. However, the commercially canned samples gained moisture by more than 13%, causing the k to increase by more than 5% and consequently increase the α .

Statistically, the two cooking treatments had similar effects on the thermal properties of potatoes (Table 6). Both treatments increased the X_{wb} but the k and ρ were not significantly affected. Although the change in k of the unblanched potatoes was higher than the standard deviation, it was not significant because it was lower than the standard deviation of the unprocessed test samples. Moreover, both cooking processes resulted in increases in c_p and decreases in α . Potatoes cooked in CPS did not absorb as much moisture as those boiled in

TABLE 4.
THERMAL PROPERTIES AND VOLUMETRIC CHANGE
OF BLANCHED AND BOILED POTATOES

	Blanched (10 min.)				Boiled (2.5 h)			
	$\bar{x} \pm E^a$	N	$\Delta, \%^b$	t-Test ^c	$\bar{x} \pm E^a$	N	$\Delta, \%^b$	t-Test ^c
X_{wb} (%, wb)	80.2±1.0	10	5.9	s	85.1±0.3	5	9.8	s
ρ (g/cc)	1.088±0.019	9	-1.7	s	1.064±0.001	5	-2.3	s
k (W/m-°K)	0.551±0.007	22	-0.7	ns	0.567±0.006	3	4.2	s
v (%)	11.0 ± 2.8	4						
c_p^d (kJ/kg-°C)	3.666 ± 0.220		3.3		3.793 ± 0.228		5.5	
α^d (m ² /s, ×10 ⁻⁶)	0.138 ± 0.009		-2.2		0.140 ± 0.009		1.1	

^a E = uncertainty, calculations of E for X_{wb} , ρ and k = standard deviation, for c_p = 6 % of c_p , and for α = calculated from eqn. 3

^b Change in values of processed with respect to raw products.

^c Based on 2-tailed t-test at $\alpha=0.05$ of raw vs processed products.

^d Calculated

water. This may be due to the lower amount of available moisture in CPS. The test samples that were preblanched prior to cooking had lower moisture intake than those that were immediately cooked. The preblanching may have caused the test sample surface to initially harden so as to decrease moisture diffusivity. However, this effect seemed temporary since as previously discussed when potatoes were boiled for an extended period, they absorbed more moisture (Table 4).

The result of the baking tests showed that k decreased significantly for potatoes that were baked for 1.5 h and longer and remained unchanged for those baked for 1 h or less (Table 7 and 8). Although the average k of potatoes baked for 1 h decreased by 1.6%, it was found to be statistically insignificant since the standard deviation was relatively high. The standard deviations of the k values

TABLE 5.
THERMAL PROPERTIES OF CANNED POTATOES

	$F_0 = 3.7$ min.				$F_0 = 23.5$ min.				COMMERCIAL			
	$\bar{X} \pm E^a$	N	$\Delta, \%^b$	t-Test ^c	$\bar{X} \pm E^a$	N	$\Delta, \%^b$	t-Test ^c	$\bar{X} \pm E^a$	N	$\Delta, \%^b$	t-Test ^c
X_{wb} (%, wb)	85.3±0.4	5	7.7	s	85.6±0.6	5	8.1	s	87.3±0.7	10	13.2	s
ρ (g/cc)	1.061±0.002	10	-1.6	s	1.065±0.002	5	-1.2	s	1.054±0.004	11	-3.2	s
k (W/m·°K)	0.569±0.007	23	0.5	ns	0.576±0.007	12	1.6	s	0.583±0.007	14	5.1	s
c_p^d (kg/kJ·°C)	3.798±0.228		4.3		3.806±0.228		4.6		3.850±0.231		7.4	
α^d (m ² /s, x10 ⁻⁵)	0.141±0.009		-2.1		0.142±0.009		-1.7		0.144±0.009		1.1	

^aE= uncertainty, calculations of E for X_{wb} , ρ and k = standard deviation, for $c_p = 6\%$ of c_p , and for $\alpha =$ calculated from eqn. 3

^bChange in values of processed with respect to raw products

^cBased on 2-tailed t-test at $\alpha = 0.05$ of raw vs processed products

^d Calculated

TABLE 6.
THE THERMAL PROPERTIES OF COOKED POTATOES

	Blanched + Cooked ^a				Cooked ^b			
	$\bar{X} \pm E^c$	N	Δ , % ^d	t-Test ^e	$\bar{X} \pm E^c$	N	Δ , % ^d	t-Test ^e
X_{wb} (%, wb)	81.4±0.3	5	5.5	s	82.2±0.4	5	6.6	s
ρ (g/cc)	1.086±0.012	5	-0.3	ns	1.089±0.011	5	-0.1	ns
k (W/m·°K)	0.557±0.010	6	-0.2	ns	0.568±0.009	5	1.8	ns
c_p^f (kg/kJ·°C)	3.697±0.222		3.1		3.718±0.223		3.6	
α^f (m ² /s, x10 ⁻⁶)	0.139±0.009		-2.9		0.140±0.009		-1.7	

^a Blanched for 10 min. in boiling water and cooked in boiling cream of potato soup (CPS) for 50 min.

^b Cooked in boiling CPS for 60 min.

^c E = uncertainty, calculations of E for X_{wb} , ρ and k = standard deviation, for c_p = 6 % of c_p , and for α = calculated from eqn. 3

^d Change in values of processed with respect to raw products.

^e Based on 2-tailed t-test at α = 0.05 of raw vs processed products

^f Calculated

of the test samples baked for 0.5 and 1 h were higher than those baked longer; indicating that those baked longer had more uniform composition and were cooked completely. Visually, the potatoes baked for 0.5 h had uncooked centers while the others had a uniform cooked color. The baking test had no significant effect on the X_{wb} of the potatoes. This indicated that the change in the k values may be the result of starch gelatinization.

Because gelatinization can lower the k of potatoes by more than 2%, it can counteract the effect of increasing X_{wb} , e.g., potatoes that were canned to $F_0=3.7$ (Table 5) and cooked in CPS (Table 6). The X_{wb} in those cases increased by >5% but the k increased by only 2%. Thermal conductivity is more sensitive to moisture increases in materials with low starch content. For example, carrots canned to an $F_0=3.7$ increased in X_{wb} by 6.7% and k by 3.5% (Table 3). In comparison, similarly processed potatoes increased in X_{wb} by 7.7%

and k by only 0.5% (Table 5). The baking results showed that gelatinization is an important factor in the k of thermally processed starchy materials. It should be included in mathematical models that are used to calculate them. It is especially important in potatoes which have k values much lower than water.

TABLE 7.
THE THERMAL CONDUCTIVITY POTATOES BAKED FOR 0.5 AND 1.0h

	0.5 h				1.0 h			
	$\bar{x} \pm E^a$	N	$\Delta, \%^a$	t-Test ^b	$\bar{x} \pm E^a$	N	$\Delta, \%^a$	t-Test ^b
X_{wb} (%, wb)	82.5±4.8	5	0.8	ns	81.9±0.6	5	0.1	ns
k (W/m-°K)	0.567±0.015	16	-0.4	ns	0.560±0.014	12	-1.6	ns

^a Change in values of baked with respect to fresh potatoes.

^b Based on 2-tailed t -test at $\alpha = 0.05$ of raw vs processed products.

TABLE 8.
THE THERMAL CONDUCTIVITY OF POTATOES BAKED FOR 1.5 AND 2.0 h

	1.5 h				2.0 h			
	$\bar{x} \pm E$	N	$\Delta, \%^a$	t-Test ^b	$\bar{x} \pm E$	N	$\Delta, \%^a$	t-Test ^b
X_{wb} (%, wb)	81.1 ± 1.0	5	-0.9	ns	81.8 ± 0.8	5	-0.1	ns
k (W/m-°K)	0.554 ± 0.010	12	-2.6	s	0.556 ± 0.009	12	-2.2	s

^a Change in values of processed with respect to the fresh potatoes in Table 7.

^b Based on 2-tailed t -test at $\alpha = 0.05$ of raw vs processed products.

The results of this study show that the values of thermal properties that provide the most conservative estimate of F_0 are those measured after potatoes have been blanched and cooked and carrots have been canned to an $F_0=3.7$ min. Conversely, the least conservative values of thermal properties are those measured for raw carrots or for potatoes boiled for a long time or canned and stored for a long time. To illustrate the significance of this study and using the analysis of Lee *et al.* (1990), if a product whose lethality is based on potato, and if the thermal properties of potatoes that had been canned and stored are used in the calculation, the process time would be underestimated by 2%. If the lethality of a product is based on carrots and if the thermal properties of raw carrots are used in the analysis, the process time would be underestimated by less than 0.5%. It should be noted that this analysis is valid only for the processes evaluated in this study.

SUMMARY AND CONCLUSIONS

The results of the study are summarized below:

- (1) Processed potatoes expand more than 10%, 4 times as much as carrots. In the development of heat and mass models for processing of potatoes, it may be necessary to include volumetric expansion as one of the variables. The determination of product loading, which is volumetric fraction of particulates in a food product, for potatoes may be based on processed materials and for carrots on raw materials.
- (2) Materials with high starch content such as potatoes, have a lower tendency to change their k values during processing. Thermal processing increases the X_{wb} of food materials and causes their k values to increase. However, it also causes starch gelatinization which decreases the k values. The combined effect of increases in X_{wb} and starch gelatinization has a stabilizing influence on k values.
- (3) Potatoes absorb less moisture in soup than in plain water. This is important in product development where product texture is one of the quality parameters.
- (4) Generally, α decreased after thermal processing since the c_p increased more than k . However, in processes where the X_{wb} increased by more than 9%, α increased due to larger increases in k than in c_p .
- (5) The results from this study show that the thermal properties of blanched and cooked potatoes and carrots canned to an $F_0=3.7$ min provide the most conservative estimate of F_0 . Conversely, the least conservative estimates are derived from potatoes that had been either boiled for a long time or canned and then stored for a long time and from raw carrots.

- (6) This study has shown that α changes with process time. In aseptic processing, this implies that α changes as the product moves along the holding tube. Depending on the state of the various materials in a product as they enter the holding tube, α could either initially decrease and then increase or just increase. In either case, a lethality calculation should be based on the properties of the material when its α is lowest.

NOMENCLATURE

CPS	Cream of potato soup
c_p, c_{pi}	Specific heat and specific heat of food component, kJ/kg-°C
D	Diameter
$E_\alpha, E_k, E_\rho, E_{cp}$	Uncertainties or errors of the various thermal properties
f_h	f-value in thermal processing, min
F_o	Lethality or sterilizing value, min
j_h	Lag factor
k	Thermal conductivity, W/m-°K
L	Length
s, ns	Statistically significant and insignificant, respectively
N	Number of replicates
r_s	Sample radius, mm
t	Test time, s
T, T_r, T_i	Temperature, retort and initial temperature, respectively, °C
V_p, V_r	Volume of processed and raw samples, respectively, cc
X_{wb}	Moisture content, % wb (wet basis)
X_i^w	Weight fraction of food component
\bar{x}	Mean
α	Thermal diffusivity, m ² /s
α'	Coefficient of region outside the confidence interval
ρ	Density, g/cc
Δ	Change in a thermal property, %
ν	Volumetric expansion, %

REFERENCES

- ADAMS, C. 1975. *Nutritive Value of American Foods*. Agriculture Handbook No. 456. Agricultural Research Service, U.S. Department of Agriculture, Washington, DC.
- CHANDARANA, D.I. and GAVIN III, A. 1989. Modeling and heat transfer study of heterogeneous foods processed aseptically. In *Proceedings of the*

- First International Congress on Aseptic Processing Tech.*, (J.V. Chambers, ed.) pp. 56–86.
- CHANDARANA, D.I., GAVIN III, A. and WHEATON, F.W. 1989. Simulation of parameters for modeling aseptic processing of foods containing particulates. *Food Technol.* 43(3), 137–143.
- CHOI, Y.H. 1985. Food thermal property prediction as effected by temperature and composition. Ph. D. Dissertation, Purdue University, W. Lafayette, IN.
- GRATZEK, J.P. and TOLEDO, R.T. 1993. Solid food thermal conductivity determination at high temperatures. *J. Food Sci.* 58(4), 908–913.
- KLINE, S.J. and McCLINTOCK, S.J. 1953. Describing uncertainties in single-sample experiments. *Mech. Eng.* 75, 3–8. [In HENRY, Z.A. (1975). *Instrumentation and Measurement for Environmental Sciences*. ASAE. St. Joseph. MI.]
- KNIBBE, P. and RAAL, R. 1987. *Int. J. Thermophysics* 8, 181. [In NIETO DE CASTRO, C.A., TAXIS, B., RODER, H. and WAKEHAM, A. (1988), *Int. J. of Thermophysics* 9(3), 293–316.]
- LAMBERG, I. and HALLSTROM, B. 1986. Thermal properties of potatoes and a computer simulation model of a blanching process. *J. Food Technol.* 21, 577–585.
- LARKIN, J.W. 1990. Mathematical analysis of critical parameters in aseptic particulate processing systems. *J. Food Process Engineering* 13, 115.
- LEE, J.H., SINGH, R.K. and LARKIN, J.W. 1990. Determination of lethality and processing time in a continuous sterilization system containing particulates. *J. Food Eng.* 11, 67–92.
- LOPEZ, A. 1987. *A Complete Course in Canning*, 12th. Ed. The Canning Trade, Baltimore, MD.
- M.W. KELLOGG Co. 1955. *Saline Water Conversion Data Book*. U.S. Dept. of Interior. [In ASHRAE (1981). *ASHRAE Handbook - 1981 Fundamentals*. ASHRAE, Atlanta, GA.]
- MOHSENIN, N.N. 1970. *Physical Properties of Plant and Animal Materials*. Gordon and Breach Science Publishers, New York.
- MURAKAMI, E.G. 1985. Thermal and hydral stresses in kidney beans during soaking. Ph.D. Dissertation. The Pennsylvania State University, University Park, PA.
- MURAKAMI, E.G. 1994. Thermal processing affects properties of shrimp and scallops. *J. Food Sci.* 59(2), 237–241.
- MURAKAMI, E.G., SWEAT, V.E., SASTRY, S.K. and KOLBE, E. 1996. Analysis of various design and operating parameters of the thermal conductivity probe. *J. Food Eng.* 30 (1-2), 209–225.

- NIETO DE CASTRO, C.A., TAXIS, B., RODER, H. and WAKEHAM, A. 1988. Thermal diffusivity measurements by the transient hot-wire technique: A reappraisal. *Int. J. of Thermophysics* 9(3), 293–316.
- PARSON, JR., J. and MULLIGAN, J. 1978. Review of Scientific Instruments 49, 1460. [In NIETO DE CASTRO, C.A., TAXIS, B., RODER, H. and WAKEHAM, A. (1988), *Int. J. of Thermophysics* 9(3), 293–316.]
- RAO, M.A., BARNARD, J. and KENNY, J. 1975. Thermal conductivity and thermal diffusivity of process variety squash and white potatoes. *Trans. ASAE* 18(6), 1188–1192.
- SASTRY, S.K. 1986. Mathematical evaluation of process schedules for aseptic processing of low-acid foods containing discrete particulates. *J. Food Sci.* 51, 1323–1328, 1332.
- SWEAT, V.E. 1974. Experimental values of thermal conductivity of selected fruits and vegetables. *J. Food Sci.* 39, 1080–1083.
- WANG, N. and BRENNAN, J. 1992. Thermal conductivity of potato as a function of moisture content. *J. Food Eng.* 17, 153–160.

F N P PUBLICATIONS IN FOOD SCIENCE AND NUTRITION

Books

MULTIVARIATE DATA ANALYSIS, G.B. Dijksterhuis
NUTRACEUTICALS: DESIGNER FOODS III, P.A. Lachance
DESCRIPTIVE SENSORY ANALYSIS IN PRACTICE, M.C. Gacula, Jr.
APPETITE FOR LIFE: AN AUTOBIOGRAPHY, S.A. Goldblith
HACCP: MICROBIOLOGICAL SAFETY OF MEAT, J.J. Sheridan *et al.*
OF MICROBES AND MOLECULES: FOOD TECHNOLOGY AT M.I.T., S.A. Goldblith
MEAT PRESERVATION, R.G. Cassens
S.C. PRESCOTT, PIONEER FOOD TECHNOLOGIST, S.A. Goldblith
FOOD CONCEPTS AND PRODUCTS: JUST-IN-TIME DEVELOPMENT, H.R. Moskowitz
MICROWAVE FOODS: NEW PRODUCT DEVELOPMENT, R.V. Decareau
DESIGN AND ANALYSIS OF SENSORY OPTIMIZATION, M.C. Gacula, Jr.
NUTRIENT ADDITIONS TO FOOD, J.C. Bauernfeind and P.A. Lachance
NITRITE-CURED MEAT, R.G. Cassens
POTENTIAL FOR NUTRITIONAL MODULATION OF AGING, D.K. Ingram *et al.*
CONTROLLED/MODIFIED ATMOSPHERE/VACUUM PACKAGING, A.L. Brody
NUTRITIONAL STATUS ASSESSMENT OF THE INDIVIDUAL, G.E. Livingston
QUALITY ASSURANCE OF FOODS, J.E. Stauffer
SCIENCE OF MEAT & MEAT PRODUCTS, 3RD ED., J.F. Price and B.S. Schweigert
HANDBOOK OF FOOD COLORANT PATENTS, F.J. Francis
ROLE OF CHEMISTRY IN PROCESSED FOODS, O.R. Fennema *et al.*
NEW DIRECTIONS FOR PRODUCT TESTING OF FOODS, H.R. Moskowitz
ENVIRONMENTAL ASPECTS OF CANCER: ROLE OF FOODS, E.L. Wynder *et al.*
PRODUCT DEVELOPMENT & DIETARY GUIDELINES, G.E. Livingston, *et al.*
SHELF-LIFE DATING OF FOODS, T.P. Labuza
ANTINUTRIENTS AND NATURAL TOXICANTS IN FOOD, R.L. Ory
UTILIZATION OF PROTEIN RESOURCES, D.W. Stanley *et al.*
POSTHARVEST BIOLOGY AND BIOTECHNOLOGY, H.O. Hultin and M. Milner

Journals

JOURNAL OF FOOD LIPIDS, F. Shahidi
JOURNAL OF RAPID METHODS AND AUTOMATION IN MICROBIOLOGY,
D.Y.C. Fung and M.C. Goldschmidt
JOURNAL OF MUSCLE FOODS, N.G. Marriott, G.J. Flick, Jr. and J.R. Claus
JOURNAL OF SENSORY STUDIES, M.C. Gacula, Jr.
JOURNAL OF FOODSERVICE SYSTEMS, C.A. Sawyer
JOURNAL OF FOOD BIOCHEMISTRY, N.F. Haard, H. Swaisgood and B. Wasserman
JOURNAL OF FOOD PROCESS ENGINEERING, D.R. Heldman and R.P. Singh
JOURNAL OF FOOD PROCESSING AND PRESERVATION, D.B. Lund
JOURNAL OF FOOD QUALITY, J.J. Powers
JOURNAL OF FOOD SAFETY, T.J. Montville and D.G. Hoover
JOURNAL OF TEXTURE STUDIES, M.C. Bourne and M.A. Rao

Newsletters

MICROWAVES AND FOOD, R.V. Decareau
FOOD INDUSTRY REPORT, G.C. Melson
FOOD, NUTRITION AND HEALTH, P.A. Lachance and M.C. Fisher

GUIDE FOR AUTHORS

If the manuscript has been produced by a word processor, a disk containing the manuscript would be greatly appreciated. Word Perfect 5.1 is the preferred word processing program. The original and THREE copies of the manuscript should be sent along with the disk to the editorial office. The typing should be double-spaced throughout with one-inch margins on all sides.

Page one should contain: the title, which should be concise and informative; the complete name(s) of the author(s); affiliation of the author(s); a running title of 40 characters or less; and the name and mail address to whom correspondence should be sent.

Page two should contain an abstract of not more than 150 words. This abstract should be intelligible by itself.

The main text should begin on page three and will ordinarily have the following arrangement:

Introduction: This should be brief and state the reason for the work in relation to the field. It should indicate what new contribution is made by the work described.

Materials and Methods: Enough information should be provided to allow other investigators to repeat the work. Avoid repeating the details of procedures that have already been published elsewhere.

Results: The results should be presented as concisely as possible. Do not use tables *and* figures for presentation of the same data.

Discussion: The discussion section should be used for the interpretation of results. The results should not be repeated.

In some cases it might be desirable to combine results and discussion sections.

References: References should be given in the text by the surname of the authors and the year. *Et al.* should be used in the text when there are more than two authors. All authors should be given in the Reference section. In the Reference section the references should be listed alphabetically. See below for style to be used.

RIZVI, S.S.H. 1986. Thermodynamic properties of foods in dehydration. In *Engineering Properties of Foods*, (M.A. Rao and S.S.H. Rizvi, eds.) pp. 133-214, Marcel Dekker, New York.

MICHAELS, S.L. 1989. Crossflow microfilters ins and outs. *Chem. Eng.* 96, 84-91.

LABUZA, T.P. 1982. *Shelf-Life Dating of Foods*, pp. 66-120, Food & Nutrition Press, Trumbull, CT.

Journal abbreviations should follow those used in Chemical Abstracts. Responsibility for the accuracy of citations rests entirely with the author(s). References to papers in press should indicate the name of the journal and should only be used for papers that have been accepted for publication. Submitted papers should be referred to by such terms as "unpublished observations" or "private communication." However, these last should be used only when absolutely necessary.

Tables should be numbered consecutively with Arabic numerals. The title of the table should appear as below:

TABLE 1.

ACTIVITY OF POTATO ACYL-HYDROLASES ON NEUTRAL LIPIDS, GALACTOLIPIDS AND PHOSPHOLIPIDS

Description of experimental work or explanation of symbols should go below the table proper. Type tables neatly and correctly as tables are considered art and are not typeset. Single-space tables.

Figures should be listed in order in the text using Arabic numbers. Figure legends should be typed on a separate page. Figures and tables should be intelligible without reference to the text. Authors should indicate where the tables and figures should be placed in the text. Photographs must be supplied as glossy black and white prints. Line diagrams should be drawn with black waterproof ink on white paper or board. The lettering should be of such a size that it is easily legible after reduction. Each diagram and photograph should be clearly labeled on the reverse side with the name(s) of author(s), and title of paper. When not obvious, each photograph and diagram should be labeled on the back to show the top of the photograph or diagram.

Acknowledgments: Acknowledgments should be listed on a separate page.

Short notes will be published where the information is deemed sufficiently important to warrant rapid publication. The format for short papers may be similar to that for regular papers but more concisely written. Short notes may be of a less general nature and written principally for specialists in the particular area with which the manuscript is dealing. Manuscripts that do not meet the requirement of importance and necessity for rapid publication will, after notification of the author(s), be treated as regular papers. Regular papers may be very short.

Standard nomenclature as used in the engineering literature should be followed. Avoid laboratory jargon. If abbreviations or trade names are used, define the material or compound the first time that it is mentioned.

EDITORIAL OFFICE: DR. D.R. HELDMAN, COEDITOR, *Journal of Food Process Engineering*, University of Missouri-Columbia, 214 Agricultural Engineering Bldg., Columbia, MO 65211 USA; or DR. R.P. SINGH, COEDITOR, *Journal of Food Process Engineering*, University of California, Davis, Department of Agricultural Engineering, Davis, CA 95616 USA.

CONTENTS

Moisture Sorption Isotherms for Karingda (*Citrullus lanatus* (Thumb) Mansf) Seed, Kernel and Hull
S.H. SUTHAR and S.K. DAS 349

Inactivation Kinetics of *Salmonella dublin* by Pulsed Electric Field
I. SENSOY, Q.H. ZHANG and S.K. SASTRY 367

Textural and Viscoelastic Changes of Canned Biscuit Dough During Microwave and Conventional Baking
B. PAN and M.E. CASTELL-PEREZ 383

Analysis of Mass Transfer in Osmotic Dehydration Based on Profiles of Concentration, Shrinkage, Transmembrane Flux and Bulk Flow Velocity in the Domain of Time and Space
Z. YAO and M. LE MAGUER 401

The Thermal Properties of Potatoes and Carrots as Affected by Thermal Processing
E.G. MURAKAMI 415